Available online at www.sciencedirect.com
SCIENCE DIRECT®
Coordination Chemistry Reviews 250 (2006) 189–211
COORDINATION CHEMISTRY REVIEWS
www.elsevier.com/locate/ccr

Review

"Dual-side" catalysts for high and ultrahigh molecular weight homopolypropylene elastomers and plastomers

Cecilia Cobzaru [a], Sabine Hild [b,*], Andreas Boger [c], Carsten Troll [a], Bernhard Rieger [a,**]

[a] *Department of Inorganic Chemistry II, University of Ulm, Albert-Einstein-Allee 11, 89069 Ulm, Germany*
[b] *Department of Experimental Physics, University of Ulm, Albert-Einstein-Allee 11, 89069 Ulm, Germany*
[c] *AO Research, Clavendelerstrasse CH-7270 Davos, Switzerland*

Received 30 December 2004; accepted 9 June 2005
Available online 10 August 2005

Contents

Abstract

Classical Ziegler–Natta catalysts are capable of producing homopolypropylenes with high isotacticities. New trends are focussed on obtaining polypropylenes with different properties through control of the polymer microstructure. Metallocene catalysts with variable structures revealed a great potential toward this challenge.

The flexibility of the indenyl ligand substitution proved to be the key in controlling the stereoerror formation. Error type and error distribution have major implications on the mean isotactic sequence length, and therefore also on the mechanical properties of the polymer products.

* Corresponding author. Tel.: +49 731 502 3016; fax: +49 731 502 3036.
** Corresponding author. Tel.: +49 731 502 3038; fax: +49 731 502 3039.
E-mail addresses: sabine.hild@uni-ulm.de (S. Hild), bernhard.rieger@uni-ulm.de (B. Rieger).

0010-8545/$ – see front matter
doi:10.1016/j.ccr.2005.06.007

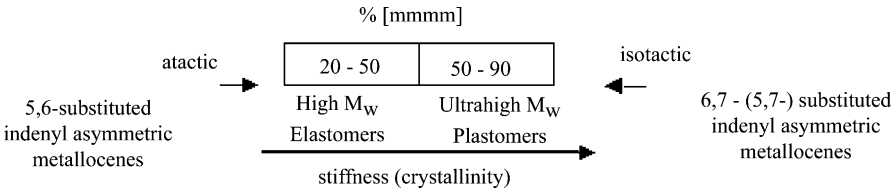

This review focuses on the synthesis of asymmetric *ansa*-metallocene catalysts, their polymerization mechanism and chain transfer reactions. The impact of the presented asymmetric *ansa*-metallocene extends beyond simple propylene polymerization disclosing a way to materials that fill the gap between "soft" thermoplastic elastomers and stiff polypropylene materials.

Keywords: Asymmetric metallocenes; Homogeneous catalysis; Polypropylenes; Thermoplastic elastomers; Plastomers

1. From elastomers to plastomers by homogeneous catalysis

1.1. Transition metal-based catalysts for propylene polymerizations

1.1.1. Metallocenes

The discovery that organic and organometallic tools can be applied for a rational catalyst design laid the foundation of worldwide activities at academia as well as in industry, leading to several types of metallocenes with precise correlation to the corresponding polymer microstructures (Fig. 1). These catalysts enable not only the synthesis of highly isotactic or more or less atactic polypropylenes but also syndiotactic, hemiisotactic and different kinds of stereoblock polymer structures, providing a portfolio of tailor-made microstructures for different industrial applications [1].

Isospecific by virtue of their symmetry [2,3], C_2-symmetric *ansa*-zirconocene catalysts produce isotactic polypropylene by enantiomorphic control. The same mechanism can be employed as a tool toward producing polymers with a wide range of isotacticities and molecular weights. Kaminsky et al. [4] designed the basic structure of the C_2-symmetric catalysts (ethylene-bridged bis(tetrahydroindenyl) zirconium complex; Fig. 1). In time, many variations of this catalyst have been realised by changing the substitutions on the cyclopentadienyl rings.

By introducing a bulkier moiety, e.g. fluorenyl in the bis(cyclopentadienyl)-based structures, a new class of catalysts was developed, known as C_s-symmetric metallocenes [5]. Due to the enantiotopic nature of their coordination positions, the chain-end control is present as the only stereocontrol mechanism leading to syndiotactic polypropenes. Highly syndiotactic polypropene [5,6] was first obtained by Ewen with C_s-symmetric catalyst $Me_2C(Cp)(9\text{-}Flu)\text{-}ZrCl_2$ [7] (Fig. 1).

Lacking any symmetry element by introducing one or more substituents in different positions of the cyclopentadienyl moiety, C_1-symmetric metallocenes possess two diastereotopic coordination sites. Thus, the stereochemistry of the polymerization reaction can be converted from the production of syndiotactic polypropene to a hemiisotactic form and even to a highly isotactic material [3]. Chien [8] reported first the synthesis of C_1-symmetric species [1-(η^5-indenyl)-1-(η^5-tetramethylcyclopentadienyl)ethane]$TiCl_2$ providing elastic polypropylenes with narrow molecular weight distribution and of fairly uniform composition. Modification of the system introduced by Chien toward dimethylsilane bridged indenyl–cyclopentadienyl zirconium or hafnium complexes by Collins et al. [9,10] (**1**, Fig. 2) afforded an improved activity and higher molecular weights ($M_w \sim 49\,000$ g/mol with hafnium complex). In analogy to the work of Chien, the elastic properties of these new materials were attributed to blocklike structures composed of isotactic and atactic sequences.

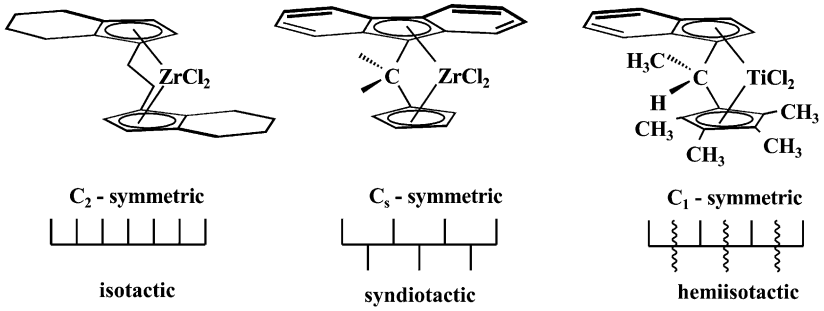

Fig. 1. Correlation of the polymer microstructure with the catalyst symmetry.

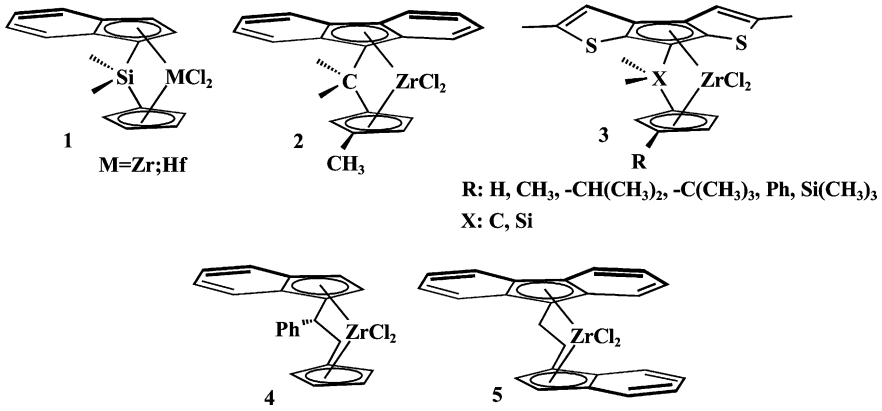

Fig. 2. Asymmetric catalysts for the production of elastomeric polypropylenes investigated by different research groups.

Ewen et al. [7,11] reported the first effectively hemiisospecific metallocene catalyst [2-(9-η^5-fluorenyl)-2-(3-methyl-η^5-cyclopentadienyl)propane] zirconium dichloride and its hafnium analogue (**2**, Fig. 2). They demonstrated that the two different coordination sites available for asymmetric metallocenes customize a broad range of material properties in migratory polyinsertion reactions of propylene by modification of the polymer microstructure. The stereochemistry of the polymerization reaction can be changed from the production of syndiotactic polypropene to a hemiisotactic form and even to a highly isotactic material by opening or blocking selective and nonselective sides in successive insertion steps. The highest molecular weights ($M_w \sim 200\,000$–$300\,000$ g/mol) are obtained with the hafnium analogue whereas the zirconium complex gives lower molecular weights ($M_w \sim 50\,000$ g/mol). Fink [5] investigated the effect of other alkyl groups (ethyl and isopropyl) in the position 3 of the cyclopentadienyl ring. Both systems have been calculated to have one nonenantioselective geometry (polymer chain in more crowded region) and one enantioselective geometry (polymer chain in less crowded region). These catalytic systems proved to be hemiisospecific, producing elastomeric polypropylenes [12].

Recently, Resconi et al. [13,14] described the use of C_1-symmetric *ansa*-zirconocenes based on substituted cyclopentadienyl or indenyl–dithienocyclopentadienyl (**3**, Fig. 2). These methylaluminoxane (MAO) activated zirconocenes produce fully regioregular polypropylenes with relatively high molecular weights ($M_v \sim 500\,000$), which, depending on the pattern of indene substitution, have largely variable degree of isotacticity and melting temperatures (T_M from 80 up to 160 °C).

Novel C_1-symmetric ethylene-bridged (Ind-Ph-Cp) and (Ind-H-Flu) complexes (**4** and **5**, Fig. 2) have been investigated [15]. Similar to complex **1**, complex **4** is provided with only one sterically demanding β-CH-substituent (indenyl-4H) allowing facile monomer coordination at each catalyst side. Consequently, the polymer stereoregularity is influenced only by the polymerization temperature. Complex **5**, on the other hand, with two opposed β-substituents (fluorenyl-5H and indenyl-4H), showed for the first time a strong dependence of stereoselectivity on monomer concentration. Thus, these unique species with two aryl groups on one side introduced the possibility to influence the rate and the position of stereoerror formation along the chain by a second parameter, different from temperature, which can be easily controlled. The fact that the content of the [mmmm] pentads in the polymers, prepared with complex **4**, remained unchanged with variations of monomer concentration was explained on the basis that only one β-substituent is not sufficient to define a chiral cage which is tight enough to favor a single transition state geometry. Hence, the polymer stereoregularities are low ([mmmm] ∼ 40%). Further research showed that this concept can be used for an arbitrary control of the crystalline/non-crystalline segments within an isotactic polymer chain and hence to conduct phase separation phenomena leading to stereoregular polyolefins with new material properties.

1.1.2. Stereocontrol of propylene polymerization via ansa-asymmetric catalysts

A theoretical investigation of the stereoselectivity dependence of the asymmetric complex **5** on the monomer concentration was recently reported by Guerra et al. [16] A significant feature of the structure of the asymmetric catalysts is the presence of the two distinct catalytic sites diastereotopically related to each other [5,17] (Fig. 3). Therefore the monomer insertion can occur at either site with different stereochemistry, one site being stereospecific whereas the other is aspecific or even counter specific. Coordination at the isospecific site leads to an isospecific migratory insertion (**A** → **B**). The catalyst, now in its aspecific state, can either interconvert to its isospecific state through a back-skip of the polymer chain (**B** → **C**), or the coordination of a new monomer can lead to an aspecific monomer insertion (**B** → **D**). If the chain back-skip reaction from the aspecific state to the isospecific state is faster than the coordination/insertion of a monomer at the aspecific state, several isospecific insertions will occur, while consecutive insertions at the aspecific state would account for the formation of atactic sequences.

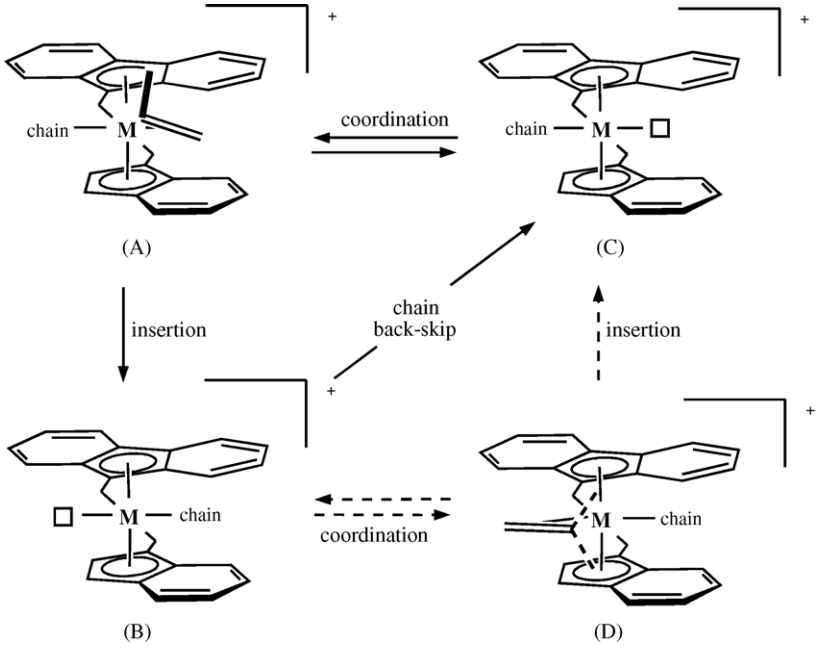

Fig. 3. Monomer coordination, insertion and chain back-skip of two diastereomeric catalytic centers.

The presence of two active polymerization sites on the same metal center of metallocene catalysts, sites that can be different in shape or symmetry, enable a much larger set of possible polymer microstructures than any other catalyst. In addition, as metallocenes are discrete molecules whose molecular structures can be studied in detail, the shape of the active sites can be tuned in order to obtain the desired type and degree of stereoregularity [5].

1.1.3. Polymer microstructures and material properties

The particular features of the asymmetric catalysts make it possible to correlate metallocene structures with polymer properties such as stereochemical microstructure and mechanical properties (Fig. 4). Polymeric products with lower tacticity (20–50% [mmmm]) display typical mechanical elastomer behavior as demonstrated by stress–strain curves. Once values of the tacticity increase (50–90% [mmmm]), the elasticity of the polymers declines in favor of increasing rigidity. As a consequence, these materials exhibit low elastic recoveries. This review will focus on complexes with asymmetric structures of the indenyl–fluorenyl type, designed to tailor the microstructures of the resulting polypropylenes so that the portfolio of the material properties is extended from low isotactic elastomers toward ultrahigh molecular weight isotactic plastomers.

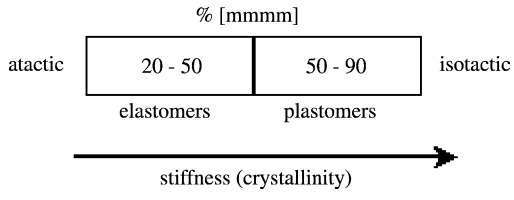

Fig. 4. Correlation of the tacticity of polymers with material properties.

2. Isotactic elastomeric polypropylenes by C_1-symmetric metallocenes

Besides C_2-symmetric catalysts, particular attention has been paid to the need to also provide asymmetric catalysts producing polypropylenes with variable isotacticities so that the resulting materials can behave as elastomers or plastomers [5]. This chapter deals with the synthesis of different *ansa*-asymmetric catalysts and the interpretation of polymerization data in terms of catalytic activity, molecular weight and tacticity of the resulting elastomeric polymers. The influence of different parameters such as polymerization temperature and monomer concentration on stereoselectivity enabled us to establish the polymerization mechanism. The difference found in the microstructures of the polymers when using different activation methods led to the hypothesis of an additional reversible chain transfer to aluminum by activation with MAO.

2.1. Homogeneous asymmetric catalysts for propylene polymerization

The initial ideas for the design of C_1-symmetric *ansa*-metallocenes for elastomeric polymers consisted in the ethylene-bridged diastereoisomers **6a** and **6b** [18] (Fig. 5) with bulky bridge substituents that stabilize the conformation of metallacycles. The highly stereoselective δ-forward conformer **6a** [15] shows, like the unsubstituted derivative **5**,

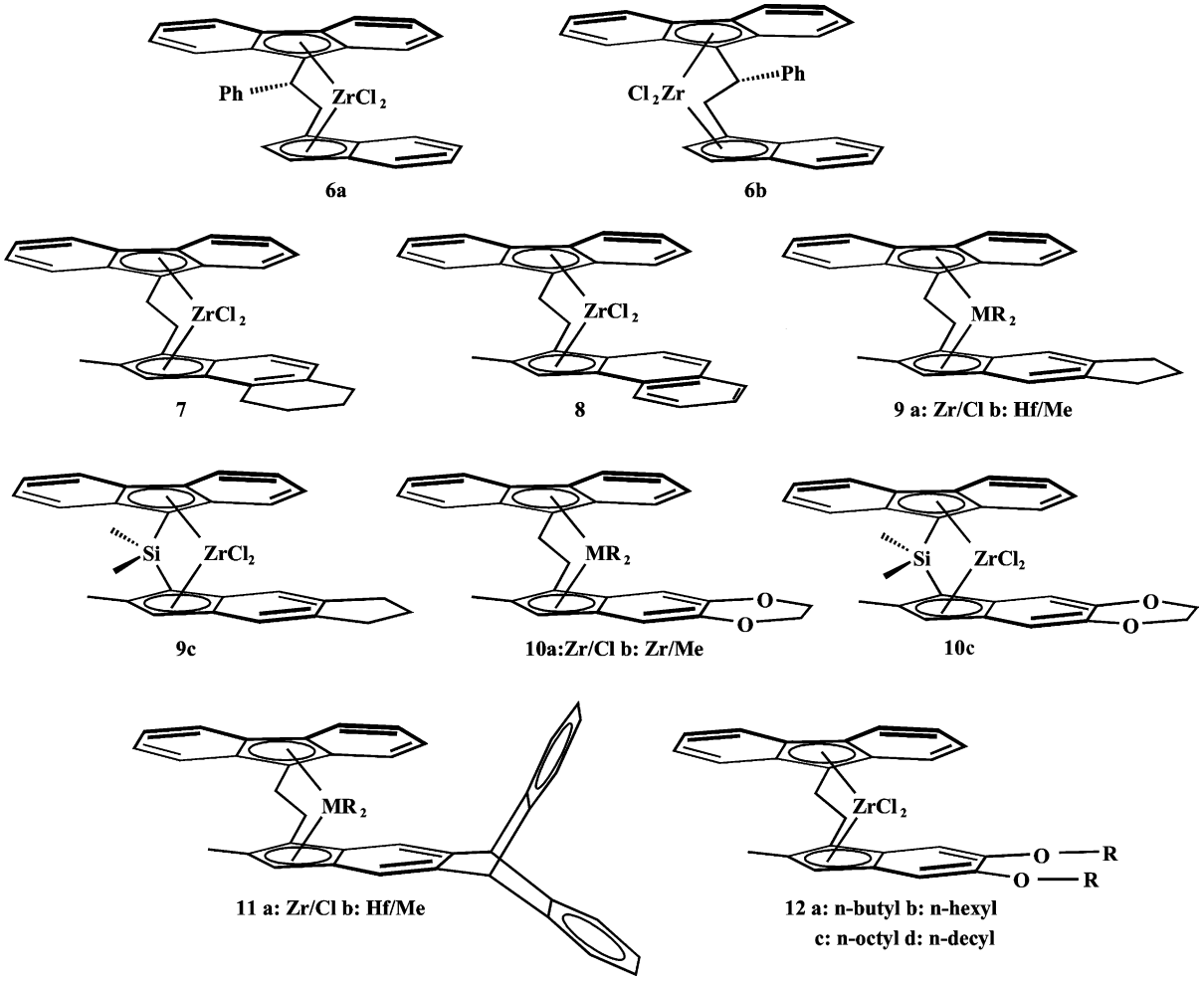

Fig. 5. Substituted ethylene- and dimethylsilane-bridged indenyl–fluorenyl zirconium complexes.

a strong decline of the stereoselectivity with the increase in propylene concentration, whereas the λ-backward conformer **6b** is nearly independent of monomer conformation. This phenomenon [16] has been attributed to energy differences (2–3 kcal mol^{-1}) for propylene coordination to the less hindered (favored) and to the more highly substituted side (nonfavored), depending on the bridge conformation. Since catalysts like **5**–**6a**,**b**/MAO produce only low-molecular weight polymers with low activity, the control of stereoerror formation could not be used to tailor the microstructure of polypropylenes in such a way that new material properties can be created.

The next approach towards the preparation of elastomeric polypropylene was based on conclusions regarding the influence of the different substitution patterns on the cyclopentadienyl rings in C_2-symmetric indenyl-based catalysts [19,20]. According to these studies, the methyl substituents in 2,2′-positions give rise to a significant increase in molecular weight whereas bulky substituents in 4,4′-positions lead to catalysts with increased activity and higher degrees of isotacticities in the resulting polypropylenes. As a consequence, a new family of asymmetric metallocenes, like **7**, **8** and **9a**–**c** [18,21] (Fig. 5), bearing a 2-methyl substituent on the indenyl moiety, was developed. The catalysts resulting after MAO activation show an unexpected high and constant activity toward the polymerization of propylene (about six times higher) and lead to significantly increased molecular weight products (up to 8 times) compared to **5**, **6a**,**b**. The explanation is based on the ability of these "dual-side" complexes to combine an isoselective side with one leading predominantly to single stereoerrors within one particular species. The fact that this non-selective side can be exposed to migratory insertion reactions, depending on the monomer concentration, provided a new tool to control the amount and the distribution of single stereoerrors along an isotactic chain. The 2-methyl substituent enhances, at the same time, the molecular weight of the resulting polypropenes, so that tacticities of $20 \leq [\text{mmmm}] \leq 70\%$ can be combined with molecular weights up to 2.3×10^5 g/mol.

A matter of particular interest was to combine both, the unique polymerization properties of the C_1-symmetric metallocene catalysts with the high potential for extending the concept of ligand design by introducing heteroatoms into the ligand framework. Therefore, the oxygen-substituted

complexes **10a–c** (Fig. 5) were synthesized and tested in propene polymerization experiments using MAO and $[(C_6H_5)_3C^+][(C_6F_5)_4B^-]$ as co-catalysts [22]. By embedding the heteroatoms into a dioxane ring, it was intended to protect the heterocycle against C–O splitting reactions with MAO and thus to improve the catalyst stability. The polymerization activities of the oxygen-containing catalysts **10a**,**c**/MAO correlate closely with the total amount of MAO. A distinct increase in catalyst activity could be observed with decreasing MAO concentration ($100 \leq Al/Zr \leq 2000$). Seemingly, the polar oxygen substituents promote the approach of the Lewis acidic aluminum co-catalyst to the zirconium center and accelerate the activation reaction in the apolar polymerization medium. The incorporation of the heteroatoms into a ring system sufficiently protects the oxygen groups against MAO-induced C–O splitting and, consequently, inhibits catalyst decomposition [23]. A further significant activity increase, up to 5100 kg PP (mol Zr [C_3] h)$^{-1}$, could be observed for the catalyst **10b**/$[(C_6H_5)_3C^+][(C_6F_5)_4B^-]$ indicating that this co-catalyst [24–29] provides a maximized concentration of active Zr^{IV} centers. The decline of the molecular weights of the polypropenes at higher Al/Zr ratios shows that the chain transfer to aluminum plays a decisive role [30–34]. After borate activation of **10b**, excluding the possibility of transfer to aluminum, the values of the molecular weights increased from 3.0×10^4 up to 16.0×10^4 g/mol.

For further investigations on the influence of sterical effects on the polymerization performance of this type of dual-side catalysts, it was examined the incorporation of the sterically demanding triptycene ligand in several bridged zirconocenes and hafnocenes **11a**,**b** (Fig. 5) [35]. In comparison to the sterically less demanding 5,6-cyclopentylsubstitution, the triptycene unit leads to significantly lower tacticities and activities.

Studies of the asymmetric catalysts **12a–d** (Fig. 5), bearing 5,6-di(*n*-alcoxy)-substituted indenyl rings, revealed a significantly increased solubility in hydrocarbon solvents like hexane and heptane [36]. Propene polymerization experiments resulted in atactic materials ([mmmm] = 10–15%) with low molecular weights (M_w = 20 000–70 000 g/mol) but with higher yields (up to factor 8) than catalyst **9a** (in toluene). A probable explanation for these unexpected results might be seen in an enhanced interaction of the active sites with aluminum scavenger molecules.

2.1.1. Ligand and complex synthesis

All 2,4-substituted indene precursors were prepared by a recently published three-step procedure [21] describing a facile route to 2-methylindenes in up to 90% overall yield (Fig. 6). Starting from methacrylic acid chloride (MAC) and readily available substituted benzene derivatives, the corresponding ketones were obtained in a one-pot reaction by Friedel–Craft acylation and subsequent Nazarov cyclization. These reactions show a remarkable regioselectivity. For naphthalene and tetrahydronaphthalene, the acylation–cyclization sequence leads nearly quantitatively to the angular indanones, while in the case of the indane, almost exclusively the linear derivatives are formed. Reduction of the ketones with $LiAlH_4$ followed by the elimination of water afforded the substituted indenes as crystalline solids. Published procedures [37–39] were followed for the synthesis of the ethylene- and dimethylsilane-bridged asymmetric fluorenyl-indenyl complexes **5–12**.

2.1.2. Polymerization experiments

2.1.2.1. Polymerization activities. The experimental data of the polymerization reactions of propylene performed with the metallocene compounds of the series **5–12** after MAO or $[(C_6H_5)_3C^+][(C_6F_5)_4B^-]$ activation are summarized in Table 1 [18,21,22,35]. The polymerization activities of all species increased with raising polymerization temperature and monomer concentration. Of all *ansa*-asymmetric catalysts investigated in this study, the complexes **9a** and **9b** showed the highest activity. Activities up to 32×10^3 kg PP (mol Zr [C_3] h)$^{-1}$ (entry 18) in toluene solution or 50×10^3 kg PP (mol Zr h)$^{-1}$ (entry 21) in liquid monomer are higher, up to five times, than the activities of the corresponding complexes without any substitution of the indenyl moiety. A correlation of the polymerization activity with the total amount of MAO could be noticed for the catalysts bearing 5,6-substituted indenyl rings. Higher Al/Zr ratios led to a distinct increase in catalytic activity of the complex **9a**, whereas the activity of the oxygen containing complexes, **10a**,**c**/MAO, proved to be favored when the MAO concentration decreased ($100 \leq Al/Zr \leq 2000$). The maximum activity is reached at Al/Zr ratios of around 300:1. At higher co-catalyst concentrations excessive MAO operates as a polymerization-inhibiting agent. A further significant activity increase could be observed for the catalysts **9b**, **10b**,

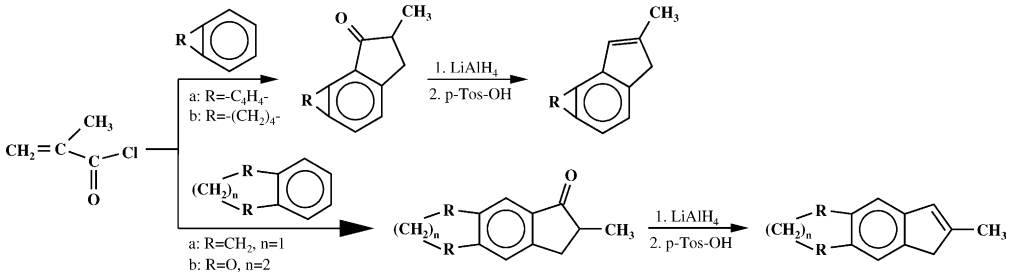

Fig. 6. Synthetic pathway leading to substituted 2-methyl indenes.

Table 1
Selected polymerization results obtained with the catalysts **5**–**12** after MAO or borate activation

Entry	Catalyst	T_p (°C)	[C_3] (mol/l)	Activity ($\times 10^3$ kg PP/mol Zr [C_3] h)	M_w ($\times 10^3$ g/mol)	Al/Zr	[mmmm] (%)
1	**5**	50	0.4	1.26	n.d.[a]	2000	68.1
2		50	0.7	2.66	28	2000	63.9
3		50	1.8	4.06	n.d.	2000	42.8
4		70	0.7	5.69	19	2000	59.3
5		50	1.9	3.59	33	2000	39.8
6	**7**	50	0.4	2.67	15	4300	79.5
7		50	1.1	6.41	22	8600	78.0
8		50	1.9	7.04	43	4300	78.4
9		70	1.1	8.87	20	4300	78.6
10	**8**	50	0.4	5.37	19	3400	72.6
11		50	1.1	6.42	38	3400	74.4
12		50	1.9	7.81	55	3400	74.7
13		70	1.1	12.54	33	3400	66.3
14	**9a**	30	1.1	2.88	71	575	47.8
15		50	0.4	8.85	54	1700	72.1
16		50	1.1	10.57	43	2300	63.9
17		50	1.9	13.01	48	2300	59.6
18		70	1.1	32.02	25	3400	64.0
19	**9b**[b]	0	C_3H_6(l)	6.0	4900	–	17.0
20		20	C_3H_6(l)	23.0	1600	–	24.0
21		50	C_3H_6(l)	50.0	700	–	34.0
22	**9c**	30	1.2	0.5	103	2000	61.6
23		30	3.0	0.5	132	2000	50.6
24		30	5.1	0.7	158	2000	44.0
25		50	3.0	1.1	85	2000	67.4
26	**10a**	30	3.0	1.0	65	100	34.7
27		30	3.0	1.2	60	300	33.5
28		30	3.0	0.7	45	1000	34.7
29		30	3.0	0.5	30	2000	35.7
30		30	5.1	1.5	115	300	35.4
31	**10b**[b]	30	1.2	5.1	135	–	55.6
32		30	3.0	2.9	150	–	42.5
33		30	5.1	3.1	160	–	36.8
34	**10c**	30	3.0	0.6	90	200	54.1
35		30	3.0	0.5	75	500	53.3
36		30	3.0	0.1	50	1000	53.0
37		30	3.0	0.15	55	2000	51.5
38		50	3.0	3.8	70	500	65.1
39	**11a**	30	1.3	0.7	45	2000	26.0
40		30	3.0	0.8	63	2000	18.0
41		30	5.1	1.0	78	2000	15.0
42		50	3.0	4.0	42	2000	35.0
43	**11b**[b]	30	1.3	2.4	153	–	23.0
44		30	3.0	1.3	262	–	20.0
45		30	5.1	2.4	295	–	19.0
46	**12a**[b]	30	1.3	0.8	20	–	11.3
47		30	3.0	0.7	50	–	10.0
48		50	3.0	1.7	40	–	12.0

[a] Not depicted.
[b] Borate activation.

11b/[$(C_6H_5)_3C^+$][$(C_6F_5)_4B^-$] indicating that this co-catalyst provides a maximized concentration of active centers.

Unlike C_2-symmetric *ansa*-metallocenes [40], the Si-bridged asymmetric complexes (**9c**) exhibit lower polymerization activities (0.5×10^3 kg PP (mol Zr [C_3] h)$^{-1}$, entry 22) than their ethylene-bridged analogues (**9a**) (2.9×10^3 kg PP (mol Zr [C_3] h)$^{-1}$, entry 14). A fast decomposition of these complexes – especially at elevated temperatures – is the explanation for the lower productivities observed.

2.1.2.2. Molecular weights. The molecular weights of the polypropylenes obtained with the catalysts **7**–**10** decrease at higher AL/Zr ratios (Table 1). This decline shows again that chain transfer to aluminum plays a decisive role [30–33], in line with the above discussion about catalysts activities. After borate activation of **9b**, **10b**, **11b**, excluding the possibility of transfer to aluminum, the molecular weights improved.

The methyl substitution in 2-position and the substituents on the indenyl moiety also lead to an increase in molecular weight compared to the unsubstituted complex **5**. The

linearly substituted complexes **9**–**11**, which carry the substituents at the 5,6-positions of the indenyl ring, produce polymers with higher molecular weights than the angularly substituted complexes **7** and **8**. Of the linearly substituted complexes, after MAO activation, the dimethylsilane-bridged derivatives, **9c** and **10c**, lead to polypropylenes with higher molecular weights. Lowering the polymerization temperatures (at constant monomer concentration) and enhancing the monomer concentration (at constant polymerization temperature) leads to an increase of the molecular weights.

2.1.2.3. Stereoselectivity. The [mmmm] pentad concentration of the polymer products resulting from **7**–**12** varies over a broad range (10–80%, Table 1), depending on the temperature, monomer concentration and bridging unit. The catalysts bearing a substitution in 4-position of the indenyl ring, **7** and **8**, lead to polymers with increased isotacticities (66–80%), as equally observed for C_2-symmetric catalysts [5]. The 5,6-substituted catalysts produce polymers with moderate [mmmm] pentad concentrations. Slightly increased isotacticities are found for dimethylsilane-bridged zirconocenes **9c** and **10c** in comparison with their ethylene-bridged analogues.

The polymerization temperature has a direct influence on the polymer isotacticity. For the catalysts **7**–**9** and **11a** an increase in stereoselectivity is observed by raising the polymerization temperature from 50 to 70 °C (at constant monomer concentration of 1.1 mol/l) for complex **7** or from 30 to 50 °C (at a constant monomer concentration of 3.0 mol/l) for complexes **9**, **11a** and **12a**. A decrease in isotacticity is observed for the polymers produced with **8**. A stronger influence of the polymerization temperature was shown to affect the linearly substituted catalysts **9a**–**c** for which the isotacticity is increased from 48% (at 30 °C) to 64% (at 50 °C) for catalyst **9a** and from 17% (at 0 °C) to 34% (at 50 °C) for catalyst **9b**.

Some remarks on the influence of the monomer concentration on polymers isotacticities conclude this section. Propylene concentrations from 0.4 up to 1.9 mol/l were used in polymerization experiments with complexes **7** and **8** but these concentrations showed little influence on the level of isotactic placements. This is not the case for the linearly substituted complexes **9**–**11** which exhibit a strong effect of the monomer concentration on stereoselectivity. Inspecting the data achieved (Table 1, entries 15–17, 22–24, 29–33, 39–41, 43–45) leads one to the conclusion that the stereoselectivity achieved declines at higher propylene concentrations (Fig. 7).

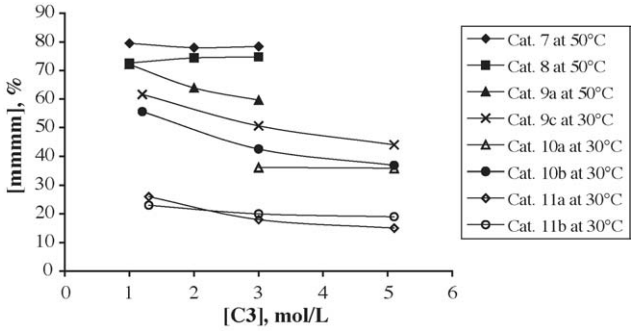

Fig. 7. Plot of polymer stereoregularity ([mmmm] pentads) vs. propene concentration ([C_3]).

2.2. Tacticity control of polypropylenes

2.2.1. Control of stereoerror formation

2.2.1.1. Proposed polymerization mechanism based on ^{13}C NMR analysis. To get a closer insight into the polymerization mechanism which is responsible for the strong dependence of stereoselectivity on monomer concentration, observed for catalysts **9a**–**c**, the pentad distribution of the polypropenes prepared with catalyst **9a** was investigated using ^{13}C NMR spectroscopy [18]. The [mmmm] pentad follows a sharp decline as the [C_3]-concentration increases. At the same time, higher monomer concentrations are correlated with higher values of all the pentads characteristic for isolated stereoerrors ([mmmr], [mmrr] and [mrrm]) (Fig. 8). A pentad distribution of [mmmr]/[mmrr]/[mrrm] = 2:2:1 for [mmmm] ≥ 40% also indicates the formation of isolated stereoerrors. Below 40% [mmmm] pentads, the [mrrr], [rrrr] and [mmrr] signals increase overproportionally, due to the fusion of isolated stereoerrors to longer stereoerror sequences. However, the content of the [rrrr] pentads is not high enough to characterize the polymers as block isotactic–syndiotactic, since the [rrrr] concentration is present in only minor quantities relative to the [mmmm] sequences.

The formation of single isolated stereoerrors is furthermore supported by the fact, that the [mrmr] pentad is absent in the polymer samples or only detectable in minor concentrations (below 1%). The same pentad is also not allowed in hemiisotactic polypropene, due to the occurrence of consecutive selective and nonselective insertions. However, none of our polymer products fits the pentad distribution required for hemiisotactic polypropene [41,42]. They can best be characterized as isotactic with variable amounts of stereoerrors that fuse to longer stereoerror sequences as isotacticity declines.

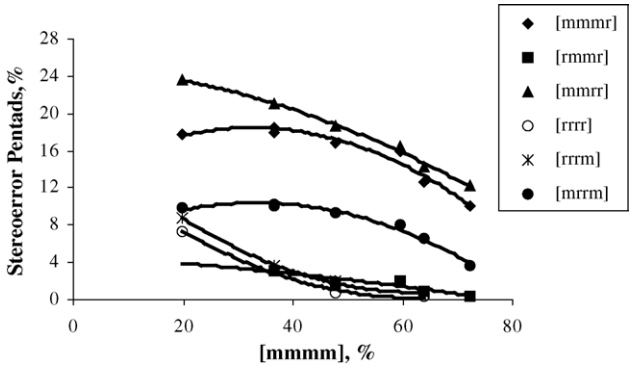

Fig. 8. Variation of stereoerrors ([mmmr], [mmrr], [mrrm], [mrrr], [rmmr], [rrrr]) in polypropenes with reduced isotacticity ([mmmm]) as a fingerprint for the polymerization mechanism.

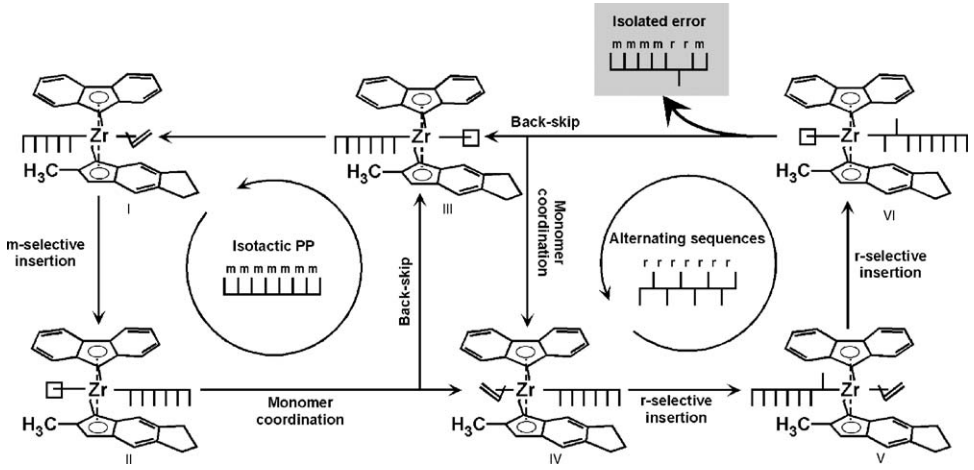

Fig. 9. Proposed mechanism for the formation of isotactic polypropenes with isolated stereoerrors obtained by these types of C_1-symmetric catalysts.

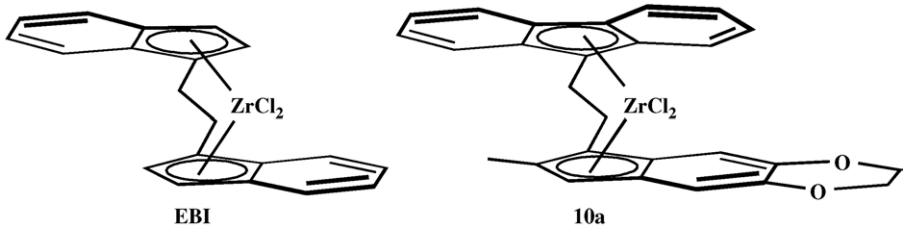

Fig. 10. EBI = ethylenebis(1-η^5-indenyl) zirconium dichloride and {1-[5,6-(ethylenedioxy)-2-methyl-1-η^5-indenyl]-2-(9-η^5-fluorenyl)ethane} zirconium dichloride (**10a**).

The decline of the [mmmm] pentad contents with an increasing monomer concentration were attributed to the existence of two coordination sites (Fig. 9) in these "dual-side" complexes, which show different stereoselectivities for monomer coordination and insertion.[1] This hypothesis is supported by Guerra et al. in a theoretical study [16] performed on the complexes **9a**,**b**.

The two sites available for monomer coordination are depicted in Fig. 9 along with the proposed reaction pathway that explains the formation of isotactic polypropenes with variable degrees of stereoerrors.

The incoming monomer can be coordinated between the sterically demanding fluorenyl-indenyl moieties (site **I**) or at the less hindered site of the catalyst (site **IV**). Isotactic [mmmm]-sequences are produced when the polymerization reaction is performed in the following order: **I** → **II** → **III**, that means repeated migratory insertion of the monomer coordinated at site **I** (**I** → **II**) and consecutive back-skip of the growing polymer chain to the less crowded site (**II** → **III**). The difference between the activation energies of the back-skip and the formation of the high-energy alkene coordinated intermediate (**IV**) is a decisive factor in determining the probability of back-skipping process of the polymer chain. The back-skip of the polymer chain is faster than monomer coordination at low monomer concentration. Thus, complexes **9a**,**c** afford relatively high isotacticities at low C_3-concentrations and elevated temperatures. At higher C_3-concentrations, the coordination of the monomer on the less hindered site (**IV**) is favored over back-skip of the polymer chain. Coordination of the monomer at site **IV** followed by migratory insertion leads to the formation of a stereoerror (**IV** → **V**). Insertion from **V** → **VI** proceeds in a stereoselective way and leads to the observed rr triad. At low monomer concentration, the back-skip of the polymer chain to the less encumbered site (**VI** → **III**) is favored over monomer coordination (**III** → **IV**). At site **III**, the catalyst follows the isotactic cycle **I** → **II** → **III**.

2.2.1.2. Supporting deuterium labeling studies. Besides electronics effects [43–47], for which it was assumed that they are not relevant for this type of asymmetric catalysts with different side selectivity (back-skip), chain end epimerization [48–50] could be responsible for stereoerror formation. In order to rule out this mechanism, deuterium labeling experiments on stereoerror distributions of the asymmetric zirconocene **10a** have been performed and referenced the results to EBI/MAO (Fig. 10), as a representative C_2-symmetric catalyst, typically undergoing chain end epimerization at low monomer concentrations. Such deuterium labeling studies enable differentiation between intrinsic errors that are formed by a wrong enantiofacial discrimination of the prochiral monomer and isomerization-induced errors, which result from a intramolecular rearrangement of the Zr-bound chain.

[1] Early studies [15,18] demonstrated that different conformers (**5**, **6a** and **6b**) exhibit different catalytic activities but the same mechanism.

Table 2
Polypropene pentad distribution for C_2-symmetric EBI/MAO and C_1-symmetric **10a**/MAO (T_p = 50 °C) [22]

Entry	Catalyst[a]	Monomer[b]	[Monomer] (mol/l)	Al/Zr	[mmmm] (%)	[mmrr]	[mrrm]	[D]-[mrrm]
1	EBI	C_3	0.4	3000	74	8.6	4.0	–
2	EBI	C_3	0.85	3000	80	5.6	2.9	–
3	EBI	C_3	1.9	3000	84	5.7	2.3	–
4	EBI	C_3	3.3	3000	85	4.7	1.9	–
5	EBI	[D]-C_3	0.4	1500	69	9.5	1.9	2.6
6	EBI	[D]-C_3	0.85	1500	79	6.4	2.0	1.3
7	EBI	[D]-C_3	1.3	1500	82	5.5	2.0	<0.2
8	**10a**	C_3	1.9	1000	55	14.1	6.9	–
9	**10a**	C_3	1.9	2000	53	14.2	7.1	–
10	**10a**	C_3	1.9	5000	53	14.0	7.1	–
11	**10a**	C_3	0.4	1000	60	11.7	6.0	–
12	**10a**	[D]-C_3	1.9	300	57	14.1	6.5	n.o.
13	**10a**	[D]-C_3	0.4	300	65	12.6	5.1	n.o.

[a] [Zr] = (1–2) × 10^{-5} mol/l for C_3 polymerizations, [Zr] = 3.3 × 10^{-4} mol/l for [D]-C_3 polymerizations.
[b] C_3 = propene, [D]-C_3 = 1-[D]-propene.

Table 3
Selected propylene polymerization results obtained with the catalysts **10a**,**c/MAO** and **10b**/borate

Entry	Catalyst	T_p (°C)	[C_3] (mol/l)	Activity (×10^3 kg PP/mol Zr [C_3] h)	M_w (×10^3 g/mol)	Al/Zr	[mmmm] (%)
1	**10a**	30	3.0	1.2	60	300	33.5
2	**10a**	30	3.0	0.7	45	1000	34.7
3	**10a**	30	5.1	1.5	115	300	35.4
4	**10b**	30	1.2	5.1	135	–	55.6
5	**10b**	30	3.0	2.9	150	–	42.5
6	**10b**	30	5.1	3.1	160	–	36.8
7	**10c**	30	3.0	0.5	75	500	53.3
8	**10c**	30	3.0	0.1	50	1000	53.0
9	**10c**	50	3.0	3.8	70	500	65.1

Isomerization-induced stereoerrors for **10a**/MAO have not been detected at any of the applied monomer concentrations, whereas for EBI/MAO a decrease in the monomer concentration raised the amount of [D]-[mrrm] stereoerror pentads, as expected (Fig. 11, Table 2). These observations reflect a significant difference in the mechanism of stereoerror formation between these two catalyst systems due to the different positions of the substitutions on the indenyl rings. For EBI/MAO, at low monomer concentration, the formation of the [mrrm] pentad is – to a large extent – a consequence of the isomerization of the Zr-alkyl bond. The decisive factor causing stereoerrors in **10a**/MAO at high monomer concentrations is the kinetic competition between chain back-skip and monomer coordination to the aspecific side of the catalyst structure. At low C_3 pressure, a significant fraction of stereoerrors can most likely be ascribed to a reversible transfer to aluminum.

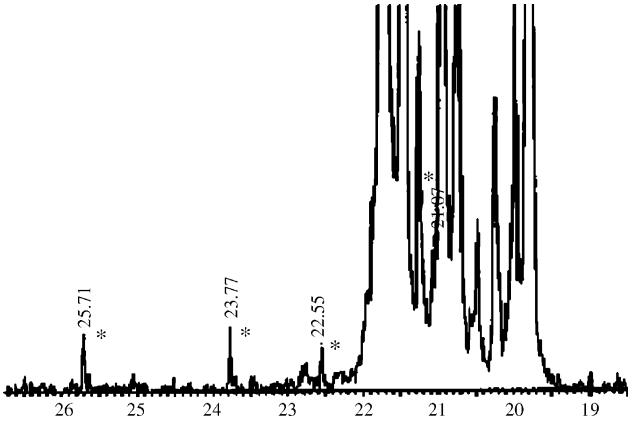

Fig. 11. ^{13}C NMR spectra of the methyl region of a polypropene sample (**10a**/MAO; T_p = 30 °C; 1.2 mol/l 1-[D]-propene); the marked peaks denote signals arising from isobutyl end groups.

Deuterium labeling studies performed with d1-propylene and catalyst **9a**[2] further support the proposed mechanism of stereoerror formation [21], explained on the basis of non-selective insertion of the prochiral monomer.

2.2.2. *Reversible chain transfer to aluminum*

2.2.2.1. Influence of the substitution. The [mmmm] pentad concentration of the polymer products resulting from 5,6-ethoxy indenyl complexes **10a**,**c** varies over a broad range (33–65%, Table 3) depending on temperature (entries 8 and 9), monomer concentration (entries 2 and 3) and bridging unit (entries 2 and 8) but is independent of the Al/Zr ratio [22]. This is a surprising observation because, in contrast to typical MAO-induced polymerizations, reduced activities at higher

[2] The dimethylsilane-bridged systems showed a relative rapid decomposition during the first minutes of the polymerization reaction [22,82]. Thus they could not be fully investigated.

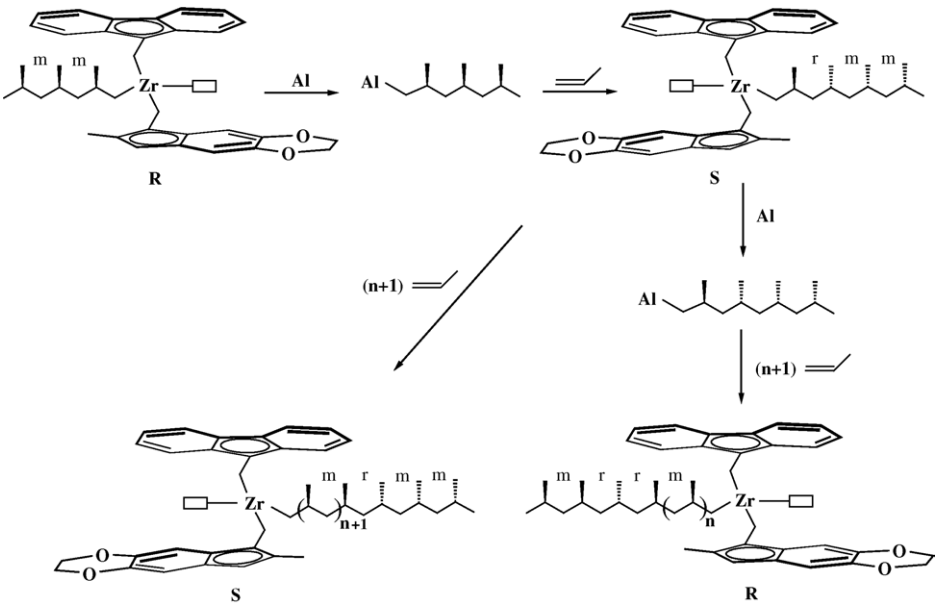

Fig. 12. The proposed mechanism of reversible chain transfer to aluminum.

aluminum contents indicate a direct interaction of MAO and Zr^{IV} centers.

As expected, the lower Al/catalyst ratio within in situ TIBA/borate activation method of **10b** leads to increased molecular weights (Table 3, entries 4–6), but also to increased isotacticities. This proves that the higher aluminum content, when using MAO as co-catalyst, does contribute to the overall stereoselectivity of the polymerization reaction.

As previously demonstrated [28,51] the co-catalysts introducing the $B(C_6F_5)_4^-$ counteranion exhibit the highest activities and stereoregularities, yielding the highest molecular weights for a given precatalyst and polymerization temperature. On the other hand, the ion-pairing tendency of $L_2ZrCH_3^+$ cations in solution (L-ligand) is a key contributor to the overall propagation rate. The stability of the ion pair for a given counterion is expected to decrease as L becomes more sterically encumbered and, thus, more reactive despite the reduced electrophilicity of the metallocenium ion [52]. Taking into account these facts one can expect that, with high sterically hindered systems as discussed in the present study, the relative rates of insertion versus chain back-skip are only slightly counterion-dependent. The differences in the polymerization data still found for the two activation methods led us to the conclusion that, besides chain "back-skip", a different mechanism occurs when using MAO-activated catalysts. Fink [53] reported the manufacture of stereoblock polymers of polypropylene by simultaneous supporting of two metallocenes with different selectivities on the same silica. These polymer microstructures were obtained due to a chain transfer between the two active species using aluminum alkyls as chain transfer agents. The transfer reaction takes place from the isotactic working species to the syndiotactic working ones as well as to another isotactic working catalyst with the same probability. Based on the above-mentioned facts, we suggested reversible chain transfer reaction as the most probable explanation.[3]

The catalytic system consists of two diastereoisomers as a result of the intrinsic chirality at the metal center [54]. Under different polymerization conditions, the coordination and insertion of the monomer can take place at the metal center of either of the two enantiomers. The reduced molecular weights of the polymer products at higher Al/Zr ratios suggest the unidirectional transfer of polymer chains from Zr^{IV} (enantiomer *R*, for example) to aluminum. Relocation from aluminum to the other enantiomer of the C_1-symmetric catalyst species (enantiomer *S*, Fig. 12) and then back to *R* would lead to the formation of a single stereoerror [mrrm] (Table 4) and could – at enhanced frequencies – account for the observed reduction of the isotacticities in case of MAO-activated complexes [53,55,56]. If the insertion of the new monomer unit takes place further at the Zr center of the enantiomer *S* then stereoerrors of type [mrmm] are found along the polymer chain.

The relatively strong decline of the polymers molecular weights (up to 20 000 g/mol) at higher Al/Zr ratios (Table 3, entries 1–2, 7–8) is one of the effects of the reversible chain transfer to aluminum at constant polymerization temperature and monomer concentration. Additionally, this mechanism could lead to different polymer microstructures in terms of the [mmrm] content. The formation of a stereodefect such as

[3] Co-catalyst effects, as reported for other C_1-symmetric catalysts [51], might be also considered for the changes in polymer microstructure. Model studies on ion pairs provided evidence for the dependence of the counter ion effects on the nature of the bridging group or metal center of the catalyst, as well as on the chain back-skip (chain end epimerization)/insertion rates. Therefore, we suggested reversible chain transfer as being responsible for different product molecular weights and microstructural features, obtained in this study, with both activators.

Table 4
Polypropene pentad distribution (%)

Entry	Catalyst	[mmmm]	[mmmr]	[rmmr]	(mmrr)	[mmrm] + [rrmr]	[rrrr]	[rrrm]	[mrrm]
26	**10a**	34.7	17.1	2.1	19.5	7.6	2.7	4.8	10.0
27	**10a**	33.5	17.6	2.5	20.4	7.5	2.2	4.7	10.1
28	**10a**	34.7	17.1	2.0	20.5	7.2	3.0	5.4	9.1
29	**10a**	35.7	17.3	2.7	21.4	7.0	3.0	3.9	8.2
30	**10a**	35.4	17.5	2.4	19.4	7.3	2.9	4.9	9.2
31	**10b**	55.6	14.8	–	15.5	2.8	–	1.4	7.5
32	**10b**	42.5	17.3	1.5	18.8	5.9	1.1	3.0	9.3
33	**10b**	36.8	18.0	3.2	19.5	6.8	3.0	4.7	8.3

[mmrm] requires two chemical steps while the chain termination (responsible for molecular weight decline) takes place in only one step. As a consequence, the variation of the [mmrm] pentad is less sensitive to Al/Zr ratios.

Based on the experimental evidence [57,58] the nature of the polymerization medium affects the stability of the active species. In accordance with these observations it is expected that the partially reduced solubility of the compounds **10a**,**b** in hydrocarbon solvents might hinder important aspects of the polymerization process. To us the necessary condition for clarifying this assumption was to study the polymerization process catalysed by similar derivatives with increased solubility in hydrocarbon solvents (hexane, heptane). The synthesis of the zirconocene derivatives containing 5,6-di(*n*-alkoxy) indenyl complexes (**12a**–**d**) provided the catalysts needed. Propylene polymerization experiments performed in toluene and heptane solutions revealed significant changes compared to their ethoxy-substituted analogues.

The resulting polypropylenes (toluene solution experiments) possess reduced molecular weights and isotacticities (Table 1, entries 46–48), even after MAO-free activation processes. These characteristics are very similar for polymerizations in heptane [36]. An explanation might be found in the amphiphilic nature of the catalyst sites bearing polar "Zr-head functions" and apolar *n*-alkoxy substituents. In apolar media this might allow a close contact of oxygen-substituted Zr centers and Al(III)-activator molecules via formation of aggregates. This would lead to a reversible chain transfer, which is accepted for analogue systems and results in reduced M_w and [mmmm] values [36]. The influence of the polymerization conditions, such as temperature and monomer concentration, on polymer tacticity suggests the same chain back-skip polymerization mechanism as followed by the asymmetric catalysts above discussed.

2.2.2.2. Differences in the chain microstructure of plastomers polymerized using different co-catalysts. Based on the polymerization data regarding the influence of the Al/Zr ratio on molecular weights and isotacticities of the polymers, it was suggested that a reversible chain transfer to aluminum could occur when MAO participates to the polymerization reaction. As a consequence, the chain microstructures of polymers with similar tacticity but obtained with different co-catalysts are expected to be different. Therefore, polypropylenes containing similar amounts of isotactic pentads [mmmm] but prepared either by using MAO (MAO 54) or borate (B 51) as co-catalyst have been studied.

Table 5
Pentads distribution (%) and lengths of isotactic blocks of the two polymer samples

Sample	[mmmm]	[rmmm]	[rr]	n_{iso}
MAO 54	54	14.5	10.6	11.4
B 51	51	15.3	11.8	10.7

It has been shown [18,35] that the polymer microstructure and the resulting properties depend on the amount of isolated stereoerrors indicated by rr defects ([mmmr]:[mmrr]:[mrrm] = 2:2:1). From their ^{13}C NMR spectra, the microstructures of the polymers MAO 54 and B 51 cannot be distinguished. Nearly equal amounts of rr triads have been found for both polymers (Table 5). Since these defects also influence the length of the isotactic sequences, then this parameter might reveal some differences.

It has been reported that the average isotactic block length n_{iso} between two isolated stereoirregular insertions can be estimated by the following equation [59]:

$$n_{iso} = 4 + \frac{2[mmmm]}{[rmmm]} \quad (1)$$

where [mmmm] is the percentage of isotactic pentads and [rmmm] is the percentage of pentads containing one syndiotactic stereoerror. Within the accuracy of the method, the isotactic block lengths determined by this equation are equal for samples with comparable amounts of isotactic pentads (Table 5). This sustains the result of triad analysis. Nevertheless, differences in the crystalline microstructure, thermal and mechanical behavior of these samples sustain the proposed mechanism of reversible chain transfer.

WAXS experiments can be used to estimate the crystallinity and the crystalline microstructure of a polymer. The measured scattering curve of a semicrystalline polymer is a combination of an amorphous halo and the crystalline WAXS curve. If crystalline and amorphous phases of the WAXS curves are separated, the ratio between the integral of the crystalline WAXS curve and integral of the whole curve, corrected for the background, determine the crys-

Table 6
Crystalline fractions determined by WAXS analysis

Sample	$X_{c,WAXS}$ (%)	α/γ	x_α (%)
MAO 54	32	38/62	12
B 51	31	28/72	7

tallinity $X_{c,WAXS}$[4] (Table 6). For the samples MAO 54 and B 51 the achieved difference in crystallinity is under one percent. This is an indication that the WAXS crystallinity of plastomeric polypropylenes depends on the total amount of isotactic pentads and on the amount of stereoerrors as well. The distribution of the isotactic blocks seemed to have minor influence.

Isotactic polypropylene can crystallize in different modifications [60–65]. Here, the α- and the γ-modifications are the most commonly formed unit cells. The α-modification is the preferred crystalline form of polypropylenes synthesized by conventional Ziegler–Natta catalysts [66,67]. High molecular weight isotactic polyproylenes prepared by metallocene catalysts preferentially crystallize in the γ-form [14,68–70,75,71]. The different polymorphic behavior of metallocene and Ziegler–Natta iPP samples can be related to the different distribution of the defects in the polymeric chains generated by the different types of catalytic systems [14,72]. Whereas in metallocene-made iPPs the distribution of defects along the chains is random, in Ziegler–Natta iPP samples the majority of defects are segregated in small fractions of poorly crystallizable macromolecules or in the more irregular portions of the chain. Therefore, much longer fully isotactic sequences can be produced, leading to the crystallization of the α-form even for a relatively high overall concentration of defects. This point out that the amount of stereo defects and the stereoerror distribution will determine the crystalline modification. Most recently, De Rosa et al. [14,73] found a linear correlation of stereo defects and stereoerror distribution and the amount of γ-form crystals. Furthermore, a dependence of the crystal modification on the isotactic block length has been reported [14,74]. Fischer and Mulhaupt showed that the γ-form is favored when isotactic blocks are present, which exhibit a block length below 40 monomers [74]. For the polymers obtained with MAO activated C_1-symmetric zirconocenes (**9b**) the amount of γ-form crystals increases linearly with decreasing isotactic block length. Hence it can be deduced that, for isotactic sequences below 20 monomers, only 10% of the present crystals features the α-form [14]. Thus, the structural analysis of iPP in particular the crystallization of the γ-form might give information about the microstructure of the polymer chain.

[4] Comparing the amorphous halos of a PP sample, which is X-ray-amorphous both at room temperature and at melting temperature, with the semi-crystalline samples after melting, revealed a goodfit to the WAXS records. This proves that the amorphous structure of the semi-crystalline samples feature the same scattering properties as a totally amorphous sample. Thus, the different amounts of scattering could be separated.

WAXS peaks can be used to discriminate between the two crystalline forms. Whereas the α-modification reveals a WAXS peak at $2\theta = 18.6^\circ$ $(130)_\alpha$, the γ-modification appears at $2\theta = 20.1^\circ$ $(117)_\gamma$. The WAXS curves of the plastomeric polypropylenes, MAO 54 and B 51, clearly show that they crystallize in mixed α/γ modification (Fig. 13). Fitting individual peaks using a Lorentzian function, as shown in the small graph in Fig. 13, can be used to estimate the fractions of the corresponding α- and γ-phases. This analysis reveals that in both samples the α-modification prevails, but in the case of using MAO as co-catalyst, higher relative amounts of the γ-modification can be found compared to polymers synthesized with borate as co-catalyst (Table 6). This gives a strong indication that higher amounts of longer isotactic sequences have been prepared when MAO was used as co-catalyst.

For isotactic polypropylene the melting temperature T_M is determined by the lamellar thickness. If all variables are held constant, thinner lamellae will melt at lower temperatures than thicker ones. Taking into account that DSC yield non-equilibrium melting data, a kinetic relationship given by Wunderlich [75] can be used to determine the lamellar thickness l:

$$l = \frac{2\sigma_e T_M^0 M}{\rho_c \Delta H_f^\circ (T_M - T_M^0)} + \frac{kT_M}{b_0 \sigma_s} \quad (2)$$

where l = average lamellar thickness in nm; σ_e = specific fold surface free energy = 100 mJ/m^2; T_M^0 = equilibrium melting temperature = 460.7 K; M = molecular weight of repeating unit = 42 g/mol; ρ_c = isotactic crystal density = 0.94 g/cm^3; ΔH_f° = molar heat of fusion = 8.79 kJ/mol; T_M = observed melting temperature; k = Boltzmann's constant = 1.38×10^{-23} J/K, b_0 = single layer thickness = helix diameter = 0.65 nm; and σ_s = specific side surface free energy. The melting temperature, molar heat of fusion, crystal density and σ_e were suggested by Wunderlich [75]. The value σ_s was arbitrarily taken to be the same as for polyethylene [59]. Thus, the observed melting transitions can be used to determine the lamellar thickness. Since crystalline isotactic polypropylene has a 3_1 helix conformation and the c-axis of the repeat unit is 0.665 nm long, the isotactic block length $n_{iso,DSC}$ corresponds to the lamellar thickness l by

$$n_{iso,DSC} = \frac{l}{b_0} \times 3 \quad (3)$$

Combining Eqs. (2) and (3) enable one to estimate the average isotactic block length when the melting temperature of the sample has been measured.

DSC curves of polypropylene plastomers with an isotacticity between 40 and 60% typically reveal three melting transitions within their DSC diagram (Fig. 14, Table 7). It is likely that the different melting transitions refer to the formation of three distinct lamellar populations of a given thickness due to a non-equal distribution of isotactic block lengths.

The melting peak (T_{M1}) appearing between 320 and 325 K and the melting peak (T_{M3}) appearing between 400 and 405 K

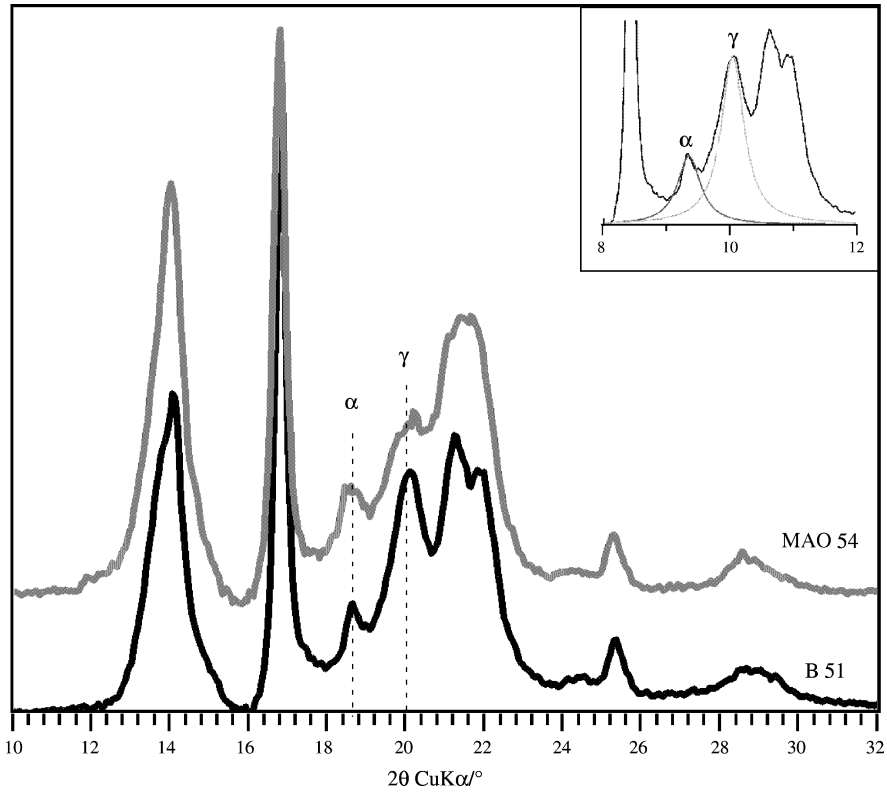

Fig. 13. The WAXS diffraction diagram show different amount of α-form and γ-form when different co-catalysts are used for the polymerization.

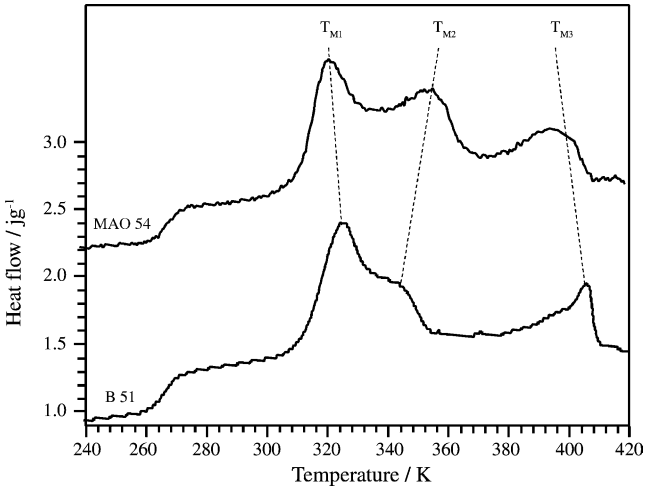

Fig. 14. DSC curves of plastomeric polypropylene prepared by different co-catalysts reveal three melting transitions.

seemed to be independent of the nature of the co-catalyst used. The first transition (T_{M1}) can be correlated to the melting of lamellae consisting of isotactic blocks, which have an average block length of about 15 isotactic monomers. This result is in good agreement with the literature [76] where it was proposed that at least 11 monomers are necessary to form crystalline lamellae. At T_{M3} melt thicker lamellae containing isotactic blocks of 37–39 consecutive monomers. Temperature-dependent WAXS experiments allow the allocation of the two transitions to the melting of either α- or γ-modification [77]. Whereas the melting of the γ-modification starts at about 320 K, γ-modification lamellae do not melt below 360 K. Thus, the thin lamellae melting at T_{M1} are crystallized in α-modification. Thicker lamellae containing longer isotactic sequences (T_{M3}) preferentially form the α-modification. These results are in good agreement with the crystalline modifications that have been proposed from the isotactic block length [14]. The quantity of a specific crystalline phase, melting at a specific temperature T_{Mx}, can be estimated from the corresponding peak area (specific heat of fusion ΔH). Comparing, for the two polypropylenes, the peaks areas at T_{M1} allow estimation of the amount of γ-

Table 7
Thermal characteristics and lengths of isotactic blocks determined by DSC

Sample	T_{M1} (K)	T_{M2} (K)	T_{M3} (K)	n_{iso2}	n_{iso3}	ΔH_{ges} (J g^{-1})	ΔH_a (J g^{-1})
MAO 54	322	356	396	21	34	48.7	8.4
B 51	322	345	405	19	39	33.9	5.7

phase crystals. The larger area observed for sample B 51 shows that higher amounts of the lamellae crystallized in a γ-modification, are present. This result supports the observations of the WAXS experiments.

In contrast, the melting transition appearing at T_{M2} reveals a clear dependence on the type of the used co-catalyst (Table 7). When MAO is used as co-catalyst, for a sample with 54% isotacticity the melting transition T_{M2} appear at 375 K. This refers to the formation of a lamellar population, which contains blocks of 25 monomers in the isotactic sequence. According to temperature-dependent WAXS measurements [77] these lamellae can crystallize in both α- and γ-phase, respectively. For the corresponding sample prepared using borate as co-catalyst, the melting transition T_{M2} appears at lower temperatures of about 345 K. This melting temperature can be correlated to the presence of lamellae containing blocks of 19 monomers. Due to temperature-dependent WAXS measurements [77], these lamellae are crystallized in γ-modification. The results points out clearly that the nature of the co-catalyst influences the length and the distribution of the isotactic blocks.

The differences in the prevailing crystalline form are reflected in the morphology of the sample. For lower isotactic polypropylenes the lamellae crystallized in α-form can be detected by an angle of 80° between the primary and the secondary branched lamellae [78]. When higher amounts of these lamellae are present cross-hatched structures can be seen [79]. In case that γ-form lamellae crystallized edge-on primarily formed α-phase lamellae, the branching angle is 41° [78]. To visualize the different polymer morphologies microtome cuts of melt pressed films are prepared because such surfaces reflect nicely the volume structure.

In Fig. 15 the topography images of plastomeric polypropylenes MAO 54 and B 51 are shown. The sample MAO 54, where MAO is used as co-catalyst, forms extended branched lamellae, which have an average thickness of about 7 ± 2 nm. According to Eq. (2) this thickness can be correlated to an isotactic block length of about 33 monomer units, which is in good agreement with the average block length estimated from DSC. Since the angle between the main direction of a branch and the lamellae is about 40° most likely the branches consist of co-crystallized α/γ-form lamellae. In contrast to this, in sample B 51 two types of lamellae can be observed that clearly differ in thickness. Lamellae with a thickness of about 15 nm act as nuclei for the secondary crystallization of shorter lamellae. Since this lamellae grow edge-on with an angle of about 81°, crystallization in the α-form can be proposed. Thus, in agreement to the results shown above, the longer isotactic sequences will crystallize in α-modification. Additionally, in between these structures 5 nm thin lamellae with an average length of about 200 nm can be seen forming a sort of an underlying lamellar network. The thickness of the lamellae refers to the presence of isotactic sequences of about 20 monomers, which may crystallize in γ-modification.

The differences in the crystalline microstructure and the morphology result in variations in the mechanical behavior, especially in the elastic recovery. Samples containing lower amount of α-form crystals are more flexible (Fig. 16). The reduced flexibility of the sample MAO 54 might be due to the extended lamellar structures, which are transformed into fibrils during mechanical deformation. This irreversible process leads to the reduced elasticity of the sample. The lamellar network present in sample B 51 seemed to be more flexible. Possibly they can be re-formed after mechanical deformation.

2.2.2.3. Activating agent. Although metallocene-based catalysts are, as soluble systems, in principle more amenable to mechanistic study than heterogeneous catalysts, it proved for a long time rather difficult to underpin the various mechanistic ideas with firm experimental evidence [80].

Materials like silica or aluminum oxides have been used for supporting the heterogeneous Ziegler–Natta systems [81]. But for asymmetric dual-side metallocenes this strategy cannot be applied [82,18]. The reason is based on the influence of the supporting material surface on the specific stereoerror formation mechanism of these new polymerization catalysts.

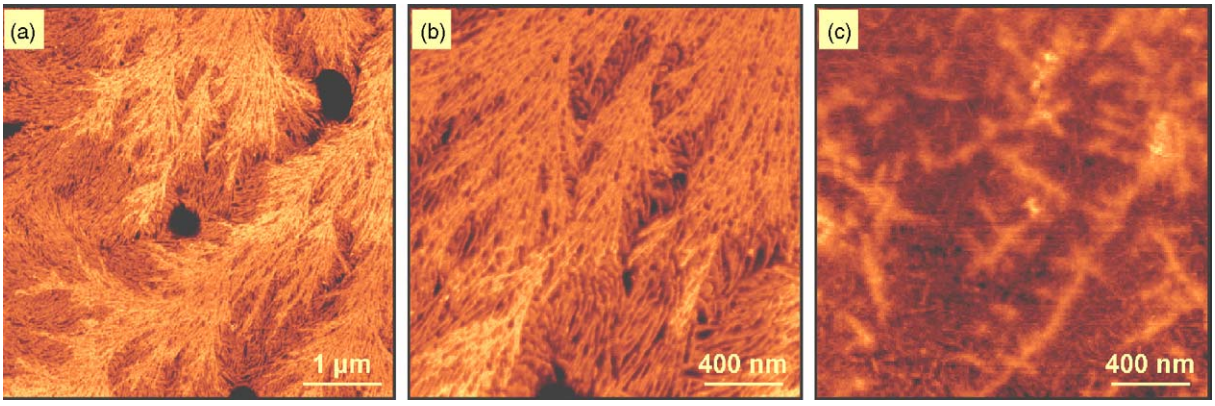

Fig. 15. Surface morphology of microtome cut polypropylene films reflect the ability of the different chain microstructures obtained for MAO (a and b) and borate (c) activation to form different lamellar super-structures.

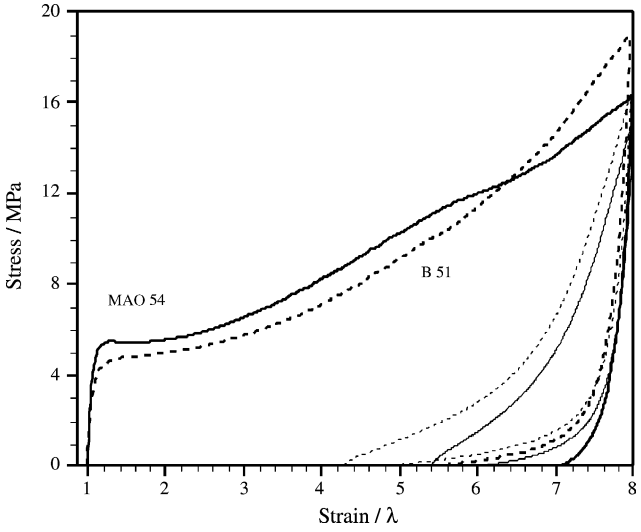

Fig. 16. Elastic recovery of polypropylene plastomers prepared using different co-catalysts (MAO 54: black line; B 51: dotted line).

Easily accessible materials, used for supporting the asymmetric catalysts, are the hyperbranched polysilanes [83]. A major advantage of the hyperbranched polymers is the distribution of functional end groups throughout their globular structure. This leads to an encapsulation of the active sites inside the polymeric matrix [84], so that the catalysts are not exclusively located on the particle surface (Fig. 17) [85]. Moreover, the nature of the functional end groups (borane) allows the study of the polymerization mechanism with a different co-catalyst.

After in situ pre-activation with an excess of triisobutylaluminum (TIBA ratio 100:1), the complex **9a** was reacted with the polymeric borane **III** to yield the active catalyst species in equilibrium (Fig. 18).

Hyperbranched polyborane co-catalysts, like **III**, are excellent activating systems for our asymmetric, "dual-side" metallocene catalysts leading to homopolypropylene elastomers with increased molecular weights, compared to solution experiments with MAO [86], due to hindered chain transfer reactions to the MAO species. Significantly increased

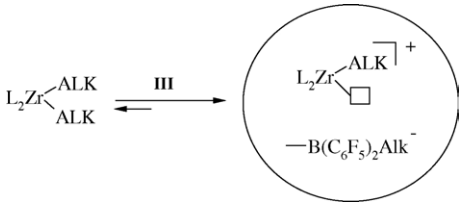

Fig. 18. Schematic activation processes with polymeric borane activator (heterogeneous).

activities were found for the polymeric activators as a consequence of the particular nature of the hyperbranched nanostructure of **III**, which leads to reduced catalyst mobility thus enhancing the concentration of the active species.

All polypropylenes are isotactic materials bearing variable [mmmm]-pentad concentrations. The isotacticities are identical to solution experiments and are found to be independent of the nature of the activating species. The occurring stereoerrors, identified by the pentad distribution, are typical for variable tacticity PP prepared with these asymmetric, dual-side catalysts, which afford increased [mmmm] pentad contents (30–50%) when the polymerization temperature is raised from 30 to 50 °C [83,87].

In contrast to conventional supports, like silica or alumina, no influence of this polymer-based supporting method on the PP microstructure was found. This lack of influence is considered as an additional advantage of the approach presented here because there is no hindrance of a solid support surface, that in most cases affects the intrinsic stereoerror formation mechanism of the particular metallocene catalyst.

3. Isotactic plastomeric polypropylenes by C_1-symmetric metallocenes

3.1. Asymmetric metallocene catalysts based on dibenzothiophene

While the asymmetric catalysts described in the previous chapters are highly active in producing high molecular

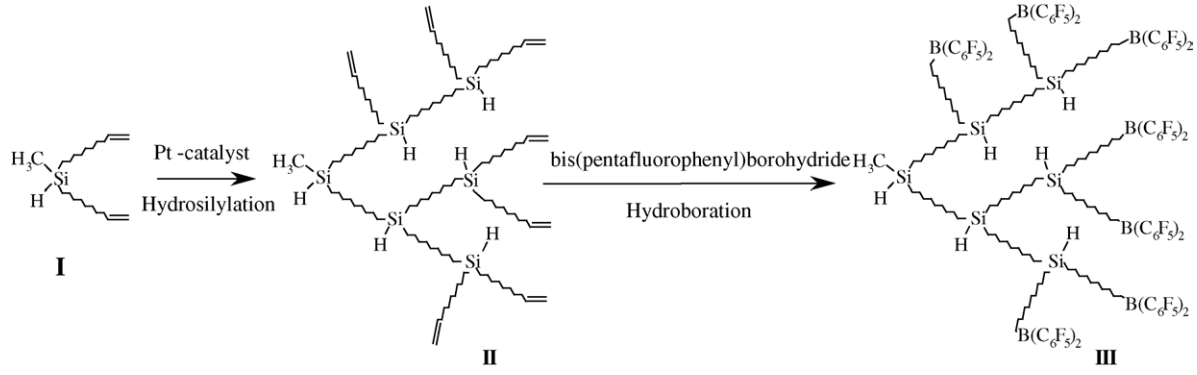

Fig. 17. Synthesis of polymethyldiundecenylsilane **II** from methyldiundecenylsilane **I** and subsequent hydroboration with bis(pentafluorophenyl) borohydride to the co-catalyst **III**.

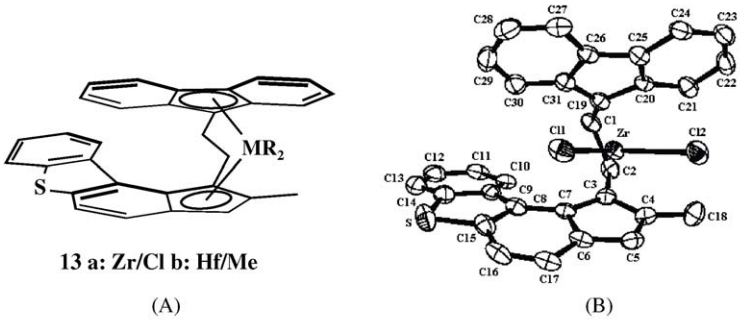

Fig. 19. Chemical structures of complexes **13a**,**b** (A) and X-ray crystal structure of complex **13a** (B) front view.

weight elastomeric polypropylenes, the production of ultrahigh molecular weight plastomers remains an area of interest. To extend the portfolio of material properties toward isotactic plastomers (less stiff polypropylene materials), it has been intended to look for other structural motifs that should maintain the excellent performance of these type of asymmetric catalysts but might afford higher tacticity values. Rigid substituents in the 6,7-positions of the 2-methylinden-1-yl fragment created a situation with a similar enantiofacial discrimination of the prochiral propylene monomer on either complex side in the migratory polyinsertion reaction. Recently it was reported the synthesis of such asymmetric, heteroatom-containing zirconocene and hafnocene complexes, **13a–c**, each bearing a substituted indenyl fragment derived from dibenzothiophene which adopts a backward orientation as shown in the investigation of the single-crystal X-ray structure [88] (Fig. 19A and B).

3.1.1. Polymerization studies

Polymerization reactions of the propylene using the zirconocenes **13a**,**b** after MAO activation have been performed. Monomer and temperature effects of these heterocenes were investigated in order to elucidate the mechanistic aspects (Table 8).

Increased catalytic activities were achieved for both complexes, **13a–c**, at higher polymerization temperatures and monomer concentrations. In the case of **13a**/MAO, the highest activity was obtained at $T_p = 60\,^{\circ}C$ (13.5×10^3 kg PP (mol Zr [C_3] h)$^{-1}$, entry 3) whereas for **13b**/borate at $T_p = 30\,^{\circ}C$ an even higher activity is observed (15.9×10^3 kg PP (mol Zr [C_3] h)$^{-1}$, entry 8). Taking into account that carbon (2.55) and sulfur (2.58) hardly differ in their electronegativities, and due to the remote position of the sulfur atom, there were no contributed activity values to electronic effects of the heteroatom.

As shown by different investigations, a sufficiently high molecular weight and isotacticities above 60% are a prerequisite for the appearance of plastomeric properties. In polymerization experiments with the 6,7-substituted complexes **13a**,**b** were obtained isotactic polypropylenes with [mmmm] pentad concentrations ranging from 65 to 85% (entry 6) and molecular weights up to 1.50×10^6 g/mol (entry 9), properties which fall in the range expected for plastomers. These achievements are unprecedented for asymmetric catalysts since the 5,6-substituted species **5–11** produced only elastomeric polypropylenes.

The isotacticity of the polypropylenes produced with **13a**/MAO is highly temperature-dependent; increasing the polymerization temperature from 30 to 60 °C causes the [mmmm] pentad concentration to decrease from 86.3 to 70.2% (entries 5 and 2). These results are in contrast to the expected chain back-skip mechanism of the asymmetric

Table 8
Polymerization results of propylene with complexes **13a**/MAO[a] and **13b**/[$(C_6H_5)_3C^+$][$(C_6F_5)_4B^-$][b]

Entry	Catalyst	Amount (μmol)	T_p (°C)	[C_3] (mol/l)	Activity[c,d]	[mmmm] (%)	M_w (kg mol^{-1})	M_w/M_n
1	**13a**	4.0	60	0.7	5.4	64.8	7	2.2
2	**13a**	3.0	60	1.6	10.4	70.2	12	2.2
3	**13a**	1.9	60	2.6	13.5	70.4	16	2.3
4	**13a**	3.0	50	1.6	9.3	77.6	22	1.9
5	**13a**	5.0	30	1.6	1.6	86.3	148	1.8
6	**13a**	2.4	30	3.0	3.6	84.9	162	2.1
7	**13a**	2.5	30	5.1	8.6	82.2	200	1.9
8	**13b**	3.7	30	C_3H_6(l)	15.9	77.7	254	2.6
9	**13b**	8.5	0	C_3H_6(l)	5.3	75.4	1524	3.8

[a] Performed in toluene, Al/Zr = 2000.
[b] Performed in liquid propylene, borate/Hf = 5.
[c] Entries 1–7 in toluene ($\times 10^3$ kg PP (mol Zr [C_3] h)$^{-1}$).
[d] Entries 8 and 9 in liquid propylene ($\times 10^3$ kg PP (mol Zr h)$^{-1}$).

zirconocenes above discussed. A change in monomer concentration has no significant influence on the tacticity of the resulted polypropylenes.

A further enhancement of the molecular weight of the plastomers obtained with **13a**/MAO was achieved performing propylene polymerizations with the hafnium dimethyl complex **13b**/[$(C_6H_5)_3C^+$][$(C_6F_5)_4B^-$]. Polymerization experiments in liquid propene showed that the molecular weight could be highly increased, in accordance with recent observations that significantly higher molecular masses could be obtained for borate-activated dimethyl complexes due to the absence of the chain transfer to aluminum [5].

3.1.2. Mechanistic considerations

In polymerization reactions with catalyst **13a**/MAO the effect of increasing stereoselectivity with decreasing temperature could be observed, leading to isotactic homopolypropylenes with [mmmm] pentad concentrations in the range of 65–85%. This is in accordance with the mechanism characteristic for C_2-symmetric metallocenes. Chien et al. [17] reported a similar behavior for *rac*-[1-(9-η^5-fluorenyl)-2-(2,4,7-trimethyl-1-η^5-indenyl)ethane] zirconium dichloride and attributed this difference in the stereoerror formation to the fact that both sides of the catalyst are stereoselective; thus isotactic polypropylene is obtained in the same manner as in the case of C_2-symmetric catalysts.

It was assumed for catalyst **13a**/MAO a similar polymerization mechanism where chain back-skip plays only a minor role and stereoerror formation is mostly due to wrong enantiofacial insertion on both sides. The pentad ratio of [mmmr]:[mmrr]:[mrrm] ≅ 2:2:1, which is typical for isospecific metallocenes operating under enantiomorphic site control, supports this "C_2-symmetry-like" polymerization behavior (Table 9).

The chemical behavior of these catalysts is strongly influenced by the orientation of the substituted indenyl fragment derived from dibenzothiophene. The thiophene fragment in the 6,7-positions of the catalysts **13a**,**b** controls the gap aperture between the fluorenyl and indenyl ligands by repulsing steric interactions at the complex backside. This leads to increased stereoselectivities (relative to **5**–**12**) and is responsible for a "C_2-symmetry-like" polymerization mechanism, characterized by increasing isotacticities when the polymerization temperature is lowered. Most importantly, the hafnium catalyst **13b**/[$(C_6H_5)_3C^+$][$(C_6F_5)_4B^-$] opens access to a novel family of polypropylene plastomers with isotacticities above 60% and ultrahigh molecular weights (up to 1.5×10^6 g/mol).

3.2. Trimethyl-indenyl-based ansa-asymmetric catalysts

3.2.1. Background and motivation

It was illustrated so far that the substitution on the indenyl ring of the asymmetric catalysts is of critical importance in determining the microstructures of the resulted polymers and the type of the polymerization mechanism. Asymmetric 5,6-cycloalkyl-substituted metallocene **9b** proved to be highly active (up to 50 000 kg PP (mol Hf h)$^{-1}$) in producing ultrahigh molecular weight homopolypropylene elastomers (between 700 000 and 5 000 000 g/mol) with low [mmmm] pentad concentrations (15 < [mmmm] < 40). Although with low activities (15.9×10^3 kg PP (mol Hf h)$^{-1}$), the heteroatom containing catalyst **13b** bearing a 6,7-substituted indenyl fragment is able to produce flexible polypropylene plastomers with isotacticities in the range from 65 to 85% and again ultrahigh molecular weights (up to 1.5×10^6 g/mol). However, especially the area of plastomeric, less stiff polypropylene homo- and copolymers was never investigated in detail, so that further improvement of the catalyst activity correlated with an easy synthetic approach was desirable. The 5,6- and 6,7-substitutions illustrated two different orientations in the polymerization mechanism and material properties. Therefore the effects of the 5,7-substitution on the polymer microstructures remained to be explored in order to elucidate the correlation between different substitution patterns of the ligand framework and the polymerization mechanism. A new asymmetric hafnocene dichloride complex, bearing a 2,5,7-trimethyl-substituted indenyl moiety (**14**, Fig. 20) was obtained following a similar reaction pathway as described in Section 2.1.1 [89].

3.2.2. Polymerization mechanism

The stereoerror formation of the C_1-symmetric complexes **5**–**12**, discussed in the present study, originates predominantly from the kinetic competition between chain back-skip and monomer coordination at the aspecific site of the

Table 9
Pentad distribution (%) for polypropylenes with **13a**/MAO[a]

Entry	[mmmm]	[mmmr]	[rmmr]	[mmrr]	[mmrm] + [rrmr] (%)	[rrrr]	[rrrm] (%)	[mrrm]
1	64.8	14.5	n.o.[b]	15.4	<1	n.o.	<1	5.3
2	70.2	12.3	n.o.	12.6	<1	n.o.	<1	4.9
3	70.4	12.7	n.o.	12.2	<1	n.o.	<1	4.7
4	77.6	9.9	n.o.	9.5	n.o.	n.o.	n.o.	3.0
5	86.3	6.0	n.o.	6.0	n.o.	n.o.	n.o.	1.8
6	84.9	6.4	n.o.	6.8	n.o.	n.o.	n.o.	1.8
7	82.2	7.0	n.o.	7.4	n.o.	n.o.	n.o.	3.4

[a] [rmrm]: entries 1–7 not observed.
[b] Pentads not observed.

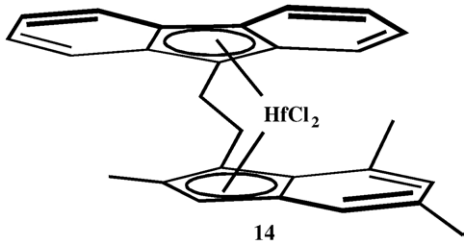

Fig. 20. 2,5,7-Trimethyl-indenyl hafnocene dichloride (**14**).

catalyst structure [15,18,21,22,82,87]. This hypothesis was confirmed studying the dependence of the polymer stereoregularity on monomer concentration and polymerization temperature. An entirely different polymerization behavior was observed for 6,7-disubstituted analogues **13a**,**b**. Although asymmetric in structure, these catalysts proved to be "C_2-symmetry-like" in polymerization mechanism which is characterized by the decrease of the polymers tacticities while increasing the polymerization temperature and declining the propylene concentration [88].

The newly designed complex **14** bears substitutions in the positions 5 and 7 of the indenyl moiety. The methyl group in position 5 resembles the front substitution existent in 5,6-substituted complexes. On the other hand, the methyl group in position 7 is expected to exhibit similar behavior as shown by 6,7-substituted compounds. As a consequence both mechanisms, chain back-skip and enantiomorphic site control, can occur.

In order to study the polymerization mechanism, the hafnocene catalyst **14**/[$(C_6H_5)_3C^+$][$(C_6F_5)_4B^-$] (preactivated with TIBA) was tested in propene polymerization experiments. Both the polymerization temperature and monomer concentration were varied and the polymerization data have been compared with the results of **13a** (Table 10).

The variation of the polymer tacticity with the polymerization temperature suggested the existence of two different polymerization mechanisms for the 6,7-substituted complex, **13a**, and the 5,7-substituted complex, **14**. The experimental data of **14** (Table 10, entries 1–2, 5–6) showed

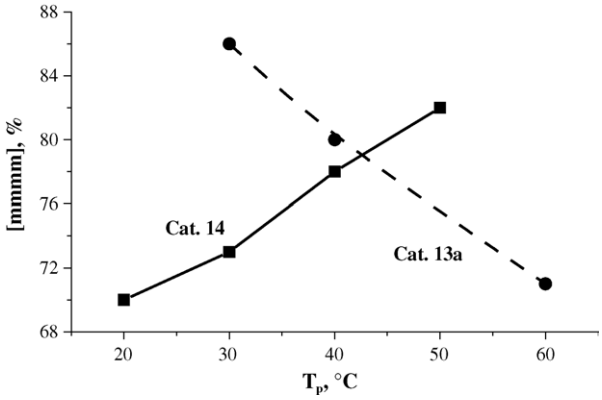

Fig. 21. Plot of the polypropylene stereoregularity vs. polymerization temperature (catalyst **14**: chain "back-skip" mechanism, catalyst **13a**: "C_2-symmetric like" mechanism).

a linear increase of the stereoselectivity (from 70 to 82%, Fig. 21) at higher polymerization temperatures. This resulted most probably from the steric interaction induced by the 5,7-dimethyl substitutions. Especially the methyl group in 5-position, which resembles the "front"-CH_2-group of the 5,6-cyclopentyl ring in **9a**, should support back-skip of the growing polymer chain before a new monomer inserts on the aspecific side of the catalyst [21] and should hence be responsible for a stereochemical control which is characteristic to all of asymmetric 5,6-substituted, high-performance polymerization catalysts.

The CH_3-substituent in 7-position of the indenyl ring, however, plays most probably the role of the thiophene fragment in the same position of catalyst **13a**, which controls the gap aperture between the bulky fluorenyl and indenyl ligands by repulsing steric interactions at the complex backside [88]. This led in **13a** to increased stereoselectivities (relative to **9a**) and was responsible for a "C_2-symmetry-like" polymerization mechanism, characterized by increasing isotacticities when the polymerization temperature is declined [5] (Fig. 21).

As expected for the chain back-skip mechanism, the stereoregularity of the polypropylenes produced with

Table 10
Polymerization data of **13a** and **14**/borate in toluene solution and liquid monomer

Entry	Catalyst	T_p (°C)	[C_3] (mol/l)	Activity ($\times 10^3$ kg PP (mol cat h)$^{-1}$)	[mmmm][a] (%)	M_w (g/mol)	M_w/M_n
1	**14**	20	4.2	127	70	860000	2.4
2	**14**	30	2.1	80	76	200000	2.8
3	**14**	30	2.9	138	74	350000	2.4
4	**14**	30	3.9	166	72	380000	2.9
5	**14**	40	2.4	151	78	130000	2.5
6	**14**	50	1.9	214	82	50000	2.6
7	**14**	10	C_3H_6(l)	39	63	960000	3.3
8	**14**	40	C_3H_6(l)	321	72	300000	3.2
9	**13a**[b]	**30**	1.6	3	86	148000	1.8
10	**13a**	30	3.0	11	85	180000	2.1
11	**13a**	30	5.1	44	82	200000	1.9
12	**13a**	50	1.6	15	78	22000	1.9

[a] Rounded values.
[b] Data from Refs. [35,88].

14/borate decreased from [mmmm] = 76% (2.1 mol C_3/l) to 72% (3.9 mol C_3/l) at increasing propene concentration. This variation supports the hypothesis that, at higher pressure, the monomer coordination at the sterically less crowded side is faster than the chain back-skip which leads to the formation of isolated stereoerrors. The tacticity values (Table 10) illustrated that, although following a similar mechanism as 5,6-substitution, the combination of 5 and 7 substitutions led to different polymer microstructures containing longer crystallizable isotactic sequences. These microstructures are assigned to plastomeric material properties.

Remarkably, the polymerization activities of the previously studied catalysts **5**–**13** were significantly improved. In toluene solution the highest productivity was reached with **14** at $T_p = 50\,^{\circ}C$ (up to 214×10^3 kg PP (mol Hf h)$^{-1}$). In liquid monomer the activity of **14** reached values even up to 321×10^3 kg PP (mol Hf h)$^{-1}$.

Higher molecular weights of the polypropylenes at lower polymerization temperatures is the trend encountered so far for asymmetric metallocene catalysts [5,18,82]. Following the same trend, ultrahigh molecular weight plastomeric polypropenes ($M_w = 8.6 \times 10^5$ g/mol at 20 °C) were obtained with **14**/borate at low polymerization temperature ($T_p = 20\,^{\circ}C$). One possible explanation was that the backward oriented 5,7-dialkyl substitution effectively suppressed the chain end epimerization process (source of stereoerrors in C_2-symmetric catalysts) and hindered at the same time a subsequent chain termination reaction, leading to higher molecular weight products [22]. On the other hand, as data have shown previously [20], high values of the molecular weights are favored by the hindrance of the chain transfer to monomer provoked by the substitution of the indenyl ligand framework of *ansa*-metallocenes in the position 2.

4. Material properties

A well-tailored polypropylene architecture is the key to control polymer properties such as stiffness and strength. With metallocene-based PP a large variety of stereoisomers can be formed using the phase separation of such stereoisomers in bulk and melt. Due to the uniform nature of metallocene-based homopolymers it became possible to establish basic correlations between molecular and supramolecular polypropylene architectures and mechanical or thermal properties.

We have shown for variable isotactic polypropylene elastomers (30% ≤ [mmmm] ≤ 60%) that the mechanical properties clearly depend on the amount of the isolated stereoerrors indicated by rr defects ([mmmr]:[mmrr]:[mrrm] = 2:2:1). [18,35,77,82,89,90]. Interesting property profiles from elastic to thermoplastic were achieved (Fig. 22). Recently, it has been shown [14] that the same effect controls the mechanical properties of highly isotactic polypropylenes (up to 97.5% [mmmm]) prepared with C_1-symmetric *ansa*-indenyl

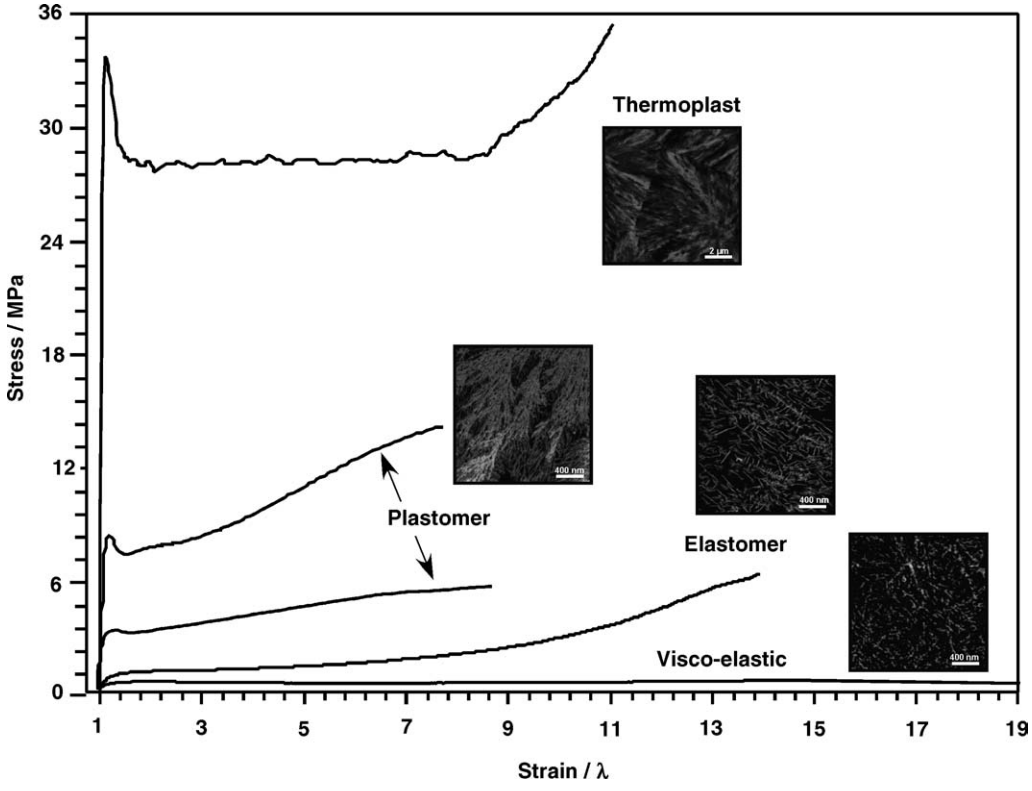

Fig. 22. Typical stress–strain curves of different types of polypropylenes.

dithienocyclopentadienyl-based zirconocenes. Different concentrations of the rr triad induce a different crystallization behavior and, consequently, afford material properties ranging from stiff to flexible plastomers.

Fig. 22 clarifies the connection between different tacticities and the material properties of the resulting polypropylenes. The length of the isotactic segments is – at increased [mmmm] pentad concentrations – long enough to afford a high degree of crystallinity so that these materials display the behavior of tough thermoplasts with relatively high melting temperatures. This behavior, specific for highly isotactic polypropylenes, is demonstrated by the higher initial strength in the stress–strain curves.

A decline in tacticity is responsible for the significant improvement of the elastic properties of the materials displaying less rigidity and more flexibility. As a consequence, for these materials lower yield points and higher maximal elongations are recorded. Materials displaying this behavior correspond to the plastomeric range of polymer properties. Unlike thermoplasts with well-defined spherulites, the crystalline phase of plastomers consists of branched lamellae. This is the case of the polymeric products obtained with catalysts **13** and **14** as a consequence of the steric effects induced by their specific backward orientation of the substitution on the indenyl moiety. Only string-like structures are formed in materials with decreased tacticity. High molecular weights combined with lower tacticity, as displayed by polymers produced with catalysts **5**–**12**, lead to a new class of elastomers. Their stress–strain curves clearly indicate a strong decline of material stiffness in comparison with the above-mentioned plastomeric and thermoplastic products. The interesting elastic property profile results not from entanglements of the polymer chain segments, but rather from a reinforcement of the amorphous phase by a crystalline network. This is validated in preliminary scanning force microscopy studies giving a first insight into the size and the distribution of crystallites needed for the formation of a stable three-dimensional network [18]. An amorphous material lacking any crystallizable sequences will form block structures and consequently exhibit low mechanical properties.

The above-mentioned facts indicate that introducing stereoerrors in an isotactic polypropylene by adjusting ligand framework and polymerization conditions, a continuous change of mechanical properties from elastic to thermoplastic can be achieved.

5. Conclusion

The combination of synthetic, structural and polymerization studies of a series of *ansa*-asymmetric catalysts has provided greater insight into the polymerization mechanism and the effectiveness of the substitution patterns on tailoring the polymer microstructures.

The existence of the two sites with different selectivities in the ligand framework proved to be a useful tool for varying the stereoregularities of the resulting polymers. In order to dictate the steric demand at each of the active sites, the nature and the position of the substitutions on the indenyl moiety have been varied. This led to a competition between monomer coordination and polymer chain migration to the less crowded site. A control over the most favored situation is achieved by changing two parameters: polymerization temperature and propylene pressure. The chain back-skip mechanism proved to be suitable in explaining the facts mentioned above. Nevertheless, a particular situation occurs when the substitution adopts a backward orientation in the ligand framework whose symmetry resembles one of the C_2-symmetric catalysts. As a consequence, the asymmetric catalysts bearing this substitution follow a polymerization mechanism found responsible for stereoerror formation with C_2-symmetric catalysts.

Two different activation methods have been used in performing the propylene polymerization experiments. The catalytic activities and molecular weights of the polymers are a sensitive function of the aluminum content provided by the activators. This dependence suggested an additional reversible chain transfer to aluminum when activating with MAO. As lower contents of Al are provided in the polymerization system in case of in situ activation with TIBA/borate, the only mechanism occurring is the chain back-skip. The differences in the polymer microstructures prepared with MAO and borate as co-catalysts are reflected in their thermal and mechanical behaviors and sustain the proposed reversible chain transfer.

Taking into consideration the correlation between polymer tacticity and material properties it was demonstrated that *ansa*-asymmetric catalysts possess a high potential for tailoring the polymer microstructures leading to new materials with properties ranging from thermoplastic elastomers to highly isotactic plastomers with ultrahigh molecular weights.

References

[1] M. Hackman, B. Rieger, CatTech 2 (1997) 79.
[2] W. Kaminsky, M. Arndt, Adv. Polym. Sci. 127 (1997) 143.
[3] H.H. Brintzinger, D. Fischer, R. Mülhaupt, B. Rieger, R.M. Waymouth, Angew. Chem. Int. Ed. Engl. 107 (1995) 1255.
[4] W. Kaminsky, K. Külper, H.H. Brintzinger, F.R.W.P. Wild, Angew. Chem. Int. Ed. Engl. 24 (1985) 507.
[5] L. Resconi, L. Cavallo, A. Fait, F. Piemontesi, Chem. Rev. 100 (2000) 1253.
[6] (a) G. Balbontin, D. Dainelli, M. Galimberti, G. Paganetto, Macromol. Chem. 193 (1992) 693;
(b) A. Galambos, M. Wolkowicz, R. Zeigler, in: E.J. Vandemberg, J.C. Salamone (Eds.), Catalysis in Polymer Synthesis, ACS Symp. Ser. 496;
(c) C. De Rosa, P. Corradini, Macromolecules 26 (1993) 5711;
(d) A.J. Lovinger, B. Lotz, D.D. Davis, M. Schumacher, Macromolecules 27 (1994) 6603;
(e) J. Rodriguez-Arnold, Z. Bu, S.Z.D. Cheng, E.T. Hsieh, T.W. Johnson, R.G. Geerts, S.J. Palackal, G.R. Hawley, M.B. Welch, Polymer 35 (1994) 1884;
(f) J. Rodriguez-Arnold, Z. Bu, S.Z.D. Cheng, J. Macromol. Sci. Rev. Macromol. Chem. Phys. C 35 (1995) 117;

(g) T. Shiomura, M. Kohno, N. Inoue, T. Asanuma, R. Sugimoto, T. Iwatani, O. Uchida, S. Kimura, S. Harima, H. Zenkoh, E. Tanaka, Macromol. Symp. 101 (1996) 289;
(h) C. De Rosa, F. Auriemma, V. Vinti, M. Galimberti, Macromolecules 31 (1998) 6206.
[7] A.J. Ewen, R.L. Jones, A. Razavi, J. Ferrara, J. Am. Chem. Soc. 110 (1988) 6255.
[8] (a) D.T. Mallin, M.D. Rausch, Y. Lin, S. Dong, J.C.W. Chien, J. Am. Chem. Soc. 112 (1990) 2030;
(b) J.C.W. Chien, G.H. Llinas, M.D. Rausch, Y. Lin, H.H. Winter, J. Am. Chem. Soc. 113 (1991) 8569;
(c) G.H. Llinas, S. Dong, D.T. Mallin, M.D. Rausch, Y. Lin, H.H. Winter, J.C.W. Chien, Macromolecules 25 (1992) 1242.
[9] (a) W.J. Gauthier, F.J. Corrigan, N.J. Nicholas, S. Collins, Macromolecules 28 (1995) 3771;
(b) W.J. Gauthier, S. Collins, Macromolecules 28 (1995) 3778.
[10] A.M. Bravakis, L.E. Bailey, M. Pigeon, S. Collins, Macromolecules 31 (1998) 1000.
[11] J.A. Ewen, M.J. Elder, R.L. Jones, L. Haspeslagh, J.L. Attwood, S.G. Bott, K. Robinson, Makromol. Chem. Macromol. Symp. 48 (48) (1991) 253.
[12] R. Kleinschmidt, M. Reffke, G. Fink, Macromol. Rapid Commun. 20 (1999) 284.
[13] I.E. Nifant'ev, I. Laishevtsev, P.V. Ivchenko, I.A. Kashulin, S. Guidotti, F. Piemontesi, I. Camurati, L. Resconi, P.A.A. Klusener, J.J.H. Rijsemus, K.P. de Kloe, F.M. Korndorffer, Macromol. Chem. Phys. 205 (2004) 2275.
[14] C. De Rosa, F. Auriema, A. Di Capua, L. Resconi, S. Guidotti, I. Camurati, I.E. Nifant'ev, I.P. Laishevtsev, J. Am. Chem. Soc. 126 (2004) 17040.
[15] B. Rieger, G. Jany, R. Fawzi, M. Steimann, Organometallics 13 (1994) 647.
[16] G. Guerra, L. Cavallo, G. Moscardi, M. Vacatello, P. Corradini, Macromolecules 29 (1996) 4834.
[17] E.J. Thomas, J.C.W. Chien, M.D. Rausch, Macromolecules 33 (2000) 1546.
[18] U. Dietrich, M. Hackmann, B. Rieger, M. Klinga, M. Leskelä, J. Am. Chem. Soc. 121 (1999) 4348.
[19] W. Spaleck, A. Antberg, J. Rohrmann, A. Winter, B. Bachmann, P. Kiprof, J. Behm, W.A. Herrmann, Angew. Chem. Int. Ed. Engl. 31 (1992) 1347.
[20] U. Stehling, J. Diebold, R. Kirsten, W. Röll, H.H. Brintzinger, S. Jüngling, R. Mülhaupt, F. Langhauser, Organometallics 13 (1994) 964.
[21] J. Kukral, P. Lehmus, T. Feifel, C. Troll, B. Rieger, Organometallics 19 (2000) 3767.
[22] J. Kukral, P. Lehmus, M. Klinga, M. Leskelä, B. Rieger, Eur. J. Inorg. Chem. (2002) 1349.
[23] I.K. Lee, W.J. Gauthier, A.M. Ball, B. Iyengar, S. Collins, Organometallics 11 (1992) 2115.
[24] (a) J.C.W. Chien, W.-M. Tsai, M.D. Rausch, J. Am. Chem. Soc. 113 (1991) 8570;
(b) J.C.W. Chien, W. Song, M.D. Rausch, J. Polym. Sci., Part A 32 (1994) 2387.
[25] X. Yang, C.L. Stern, T.J. Marks, J. Am. Chem. Soc. 116 (1994) 10015.
[26] B. Rieger, C. Janiak, Angew. Makromol. Chem. 215 (1994) 35.
[27] (a) P.A. Deck, T.J. Marks, J. Am. Chem. Soc. 117 (1995) 6128;
(b) M.A. Giardello, M.S. Eisen, C.L. Stern, T.J. Marks, J. Am. Chem. Soc. 117 (1995) 12114.
[28] E.Y.-X. Chen, T.J. Marks, Chem. Rev. 100 (2000) 1391.
[29] Z. Liu, E. Somsook, C.R. Landis, J. Am. Chem. Soc. 123 (2001) 2915.
[30] A.R. Siedle, R.A. Newmark, W.M. Lamana, J.N. Schroepfer, Polyhedron 9 (1990) 301.
[31] N. Piccolrovazzi, P. Pino, G. Consiglio, A. Sironi, M. Moret, Organometallics 9 (1990) 3098.
[32] A. Winter, J. Rohrmann, M. Antberg, W. Spaleck, W.A. Herrmann, H. Riepl, European Patent 582,195 (1994).
[33] J.A. Ewen, Macromol. Symp. 89 (1995) 181.
[34] E. Barsties, S. Schaible, M.H. Prosenc, U. Rief, W. Röll, O. Weyand, B. Dorer, H.H. Brintzinger, J. Organomet. Chem. 520 (1996) 63.
[35] S. Deisenhofer, Dissertation, University of Ulm, Ulm, 2002.
[36] M. Schlögl, B. Rieger, Z. Naturforsch. 59b (2004) 233.
[37] B. Rieger, R. Fawzi, M. Steimann, Chem. Ber. 125 (1992) 2373.
[38] B. Rieger, G. Jany, M. Steimann, R. Fawzi, Z. Naturforsch., Part B 49 (1994).
[39] Y.X. Chen, M.D. Rausch, J.C.W. Chien, J. Organomet. Chem. 497 (1995) 1.
[40] L. Resconi, R.L. Jones, A.L. Rheingold, G.P.A. Yap, Organometallics 15 (1996) 998.
[41] M. Farina, G. Di Silvestro, P. Di Silvestro, Macromolecules 15 (1982) 1451.
[42] G. Di Silvestro, P. Sozzani, B. Savare, M. Farina, Macromolecules 18 (1985) 928.
[43] J.J. Eisch, A.M. Peotrowski, S.K. Browstein, E.J. Gabe, F.L. Lee, J. Am. Chem. Soc. 107 (1985) 7219.
[44] M. Bochmann, L.M. Wilson, M.B. Huerst-House, M. Motevalli, Organometallics 7 (1998) 1148, and references given therein.
[45] G. Hlatky, H.W. Turner, R.R. Eckmann, J. Am. Chem. Soc. 111 (1989) 2728.
[46] R.F. Jordan, P.K. Bradley, N.C. Baenzinger, R.F. LaPointe, J. Am. Chem. Soc. 112 (1990) 1289.
[47] J. Lauther, R. Hoffmann, J. Am. Chem. Soc. 98 (1976) 1729.
[48] (a) M.K. Leclerc, H.H. Brintzinger, J. Am. Chem. Soc. 117 (1995) 1651;
(b) M.K. Leclerc, H.H. Brintzinger, J. Am. Chem. Soc. 118 (1996) 9024.
[49] (a) V. Busico, L. Caporaso, R. Cipullo, L. Landriani, G. Angelini, A. Margonelli, A.L. Segre, J. Am. Chem. Soc. 118 (1996) 2105;
(b) V. Busico, D. Brita, L. Caporaso, R. Cipullo, M. Vacatello, Macromolecules 30 (1997) 3971;
(c) V. Busico, R. Cipullo, L. Caporaso, G. Angelini, A.L. Segre, J. Mol. Catal. A 128 (1998) 53.
[50] (a) L. Resconi, I. Camurati, O. Sudmeijer, Top. Catal. 7 (1999) 145;
(b) L. Resconi, J. Mol. Catal. A 146 (1999) 167.
[51] (a) M. Mohammed, M. Nele, A. Al-Humydi, S. Xin, R.A. Stapleton, S. Collins, J. Am. Chem. Soc. 125 (2003) 7930;
(b) V. Busico, R. Cipullo, F. Cutillo, M. Vacatello, V.V.A. Castelli, Macromolecules 36 (2003) 4258;
(c) M.C. Chen, J.A.S. Roberts, T.J. Marks, J. Am. Chem. Soc. 126 (2004) 4605.
[52] Y.-X. Chen, M.V. Metz, L. Li, C.L. Stern, T.J. Marks, J. Am. Chem. Soc. 120 (1998) 6287.
[53] C. Przybyla, G. Fink, Acta Polym. 50 (1999) 77.
[54] K. Stanley, M.C. Baird, J. Am. Chem. Soc. 97 (1975) 6598.
[55] S. Liber, H.H. Brintzinger, Macromolecules 33 (2000) 9192.
[56] (a) J.C.W. Chien, Y. Iwamoto, M.D. Rausch, W. Wedler, H.H. Winter, Macromolecules 30 (1997) 3447;
(b) J.C.W. Chien, Y. Iwamoto, M.D. Rausch, J. Polym. Sci., Part A 37 (1999) 2439.
[57] (a) J.J. Eisch, S.I. Prombrick, G.X. Zheng, Makromol. Chem. Macromol. Symp. 66 (1993) 19;
(b) J.J. Eisch, S.I. Prombrick, G.X. Zheng, Organometallics 12 (1993) 3856.
[58] J.N. Pedeutour, K. Radhakrishman, H. Cramail, A. Deffieux, Macromol. Rapid Commun. 22 (2001) 1095.
[59] J.W. Colette, C.W. Tullock, R.N. Mac Donald, W.H. Buck, C.L. Su, J.R. Harrell, R. Mulhaupt, B.C. Anderson, Macromolecules 22 (1989) 3858.
[60] S.Z.D. Cheng, J.J. Janimak, A. Zhang, E.T. Hsieh, Polymer 32 (1991) 648.
[61] J.J. Janimak, S.Z.D. Cheng, P.A. Giusti, E.T. Hsieh, Macromolecules 24 (1991) 2253.

[62] J.J. Janimak, S.Z.D. Cheng, A. Zhang, E.T. Hsieh, Polymer 33 (1992) 728.
[63] B. Manasse, J.M. Haudin, Colloid Polym. Sci. 263 (1985) 822.
[64] R.G. Alamo, C. Chi, in: Y. Morishima, T. Norisuye, K. Tashiro (Eds.), Molecular Interactions and Time–Space Organization in Macromolecular Systems, Springer, Berlin, 1999, p. 29.
[65] R.G. Alamo, M.J. Galante, L. Mandelkern, A. Lehtinen, R. Paukkeri, J. Therm. Anal. 47 (1996) 913.
[66] R.G. Alamo, J.A. Blanco, P.K. Agarwal, J.C. Randall, Macromolecules 36 (2003) 1559.
[67] J.C. Randall, R.G. Alamo, P.K. Agarwal, C.J. Russ, Macromolecules 36 (2003) 1572.
[68] R. Thomann, S. Setz, J. Kressler, C. Wang, R. Mulhaupt, Polymer 13 (1996) 2627.
[69] S.V. Meille, S. Brückner, W. Porzio, Macromolecules 23 (1990) 4114.
[70] B. Lotz, J.C. Wittmann, A.J. Lovinger, Polymer 37 (1990) 2902.
[71] (a) C. De Rosa, F. Auriemma, C. Spera, G. Talarico, M. Gahleitner, Polymer 45 (2004) 5875;
(b) C. De Rosa, F. Auriemma, T. Boscato, P. Corradini, Macromolecules 34 (2001) 4815;
(c) F. Auriemma, C. De Rosa, Macromolecules 35 (2002) 9057;
(d) C. De Rosa, F. Auriemma, T. Cirelli, P. Longo, A.C. Boccia, Macromolecules 36 (2003) 3465;
(e) C. De Rosa, F. Auriemma, C. Perretta, Macromolecules 37 (2004) 6843.
[72] (a) C. De Rosa, F. Auriemma, T. Circelli, R.M. Waymouth, Macromolecules 35 (2002) 3622;
(b) C. De Rosa, F. Auriemma, C. Spera, G. Talarino, O. Tarallo, Macromolecules 27 (2004) 1441;
(c) G. Alamo, M.H. Kim, M.J. Galante, J.R. Isasi, L. Mandelkern, Macromolecules 32 (1999) 4050;
(d) J.C. Randall, R.G. Alamo, P.K. Agarwal, C.J. Russ, Macromolecules 36 (2003) 1572.
[73] C. De Rosa, F. Auriemma, C. Spera, G. Talarico, M. Gahleitner, Polymer 45 (2004) 5875.
[74] D. Fischer, R. Mulhaupt, Macromol. Chem. Phys. 195 (1994) 1433.
[75] B. Wunderlich, Macromolecular Physics, vol. II, Academic Press, New York, 1976, p. 149.
[76] X. Zhu, D. Yan, Y. Fang, J. Chem. Phys. B 105 (2001) 12461.
[77] A. Boger, Dissertation, University of Ulm, Ulm, 2003.
[78] S. Brückner, S.V. Meille, V. Petracone, B. Pirozzi, Prog. Polym. Sci. 16 (1991) 361.
[79] H. Schönherr, W. Wiyatno, P. Pople, C.W. Frank, G.G. Fuller, A.P. Gast, R.M. Waymouth, Macromolecules 35 (2002) 2654.
[80] M. Bochmann, J. Chem. Soc., Dalton Trans. (1996) 255.
[81] Basell's Spheripol process©; for details see: B. Rieger, R. Mülhaupt, Chimia 49 (1995) 486.
[82] G. Müller, B. Rieger, Prog. Polym. Sci. 27 (2002) 815.
[83] G.G. Hlatky, Chem. Rev. 100 (2000) 1347.
[84] For detailed information see: C. Drohmann, M. Möller, O.B. Gorbatsevich, A.M. Muzafarov, J. Polym. Sci. A 1 (38) (2000) 741.
[85] M.Q. Slagt, S.E. Stiriba, R.J.M. Klein Gebbink, H. Kautz, H. Frey, G. van Koten, Macromolecules 35 (2002) 5734.
[86] M. Schlögl, Dissertation, University of Ulm, Ulm, 2003.
[87] B. Rieger, C. Troll, J. Preuschen, Macromolecules 35 (15) (2002) 5742.
[88] S. Deisenhofer, T. Feifel, J. Kukral, M. Klinga, M. Leskelä, B. Rieger, Organometallics 22 (2003) 3495.
[89] C. Cobzaru, S. Deisenhofer, A. Harley, C. Troll, S. Hild, B. Rieger, Macromol. Chem. Phys. 206 (12) (2005) 1231.
[90] U. Dietrich, M. Hackmann, B. Rieger, Rubber Chem. Technol. 73 (2000) 839.